

Image Processing using PSPT

HAYLEY ROBERTS

MENTORS:

JERRY HARDER

MARK RAST

STEPHANE BELAND

RANDY MEISNER



Laboratory for Atmospheric and Space Physics
University of Colorado Boulder

Image Processing using PSPT

1. Relevant Sun Science

- Features of Importance
- Impact on Irradiance

2. PSPT Instrumentation



3. Flat-Fielding

- Importance of Removing Artifacts
- Methodology
- Issues behind Processing

4. Core-to-Wing Imaging in Ca II

- Methodology
- Importance behind the Data



Relevant Sun Science

SECTION 1

Earth's Energy Sources

Heat Source	Heat Flux* (W/m ²)	Relative Input
Solar Irradiance	340.25	1.00
Heat Flux from Earth's Interior	0.0612	1.80E-04
Infrared Radiation from the Full Moon	0.0102	3.00E-05
Sun's Radiation Reflected from Moon	0.0034	1.00E-05
Energy Generated by Solar Tidal Forces in the Atmosphere	0.0034	1.00E-05
Combustion of Coal, Oil, and Gas in US (1965)	0.0024	7.00E-06
Energy Dissipated in Lightning Discharges	0.0002	6.00E-07
Dissipation of Magnetic Storm Energy	6.80E-05	2.00E-07
Radiation from Bright Aurora	4.80E-05	1.40E-07
Energy of Cosmic Radiation	3.10E-05	9.00E-08
Dissipation of Mechanical Energy of Micrometeorites	2.00E-05	6.00E-08
Total Radiation from Stars	1.40E-05	4.00E-08
Energy Generated by Lunar Tidal Forces in the Atmosphere	1.00E-05	3.00E-08
Radiation from Zodiacal Light	3.40E-06	1.00E-08
Total of All Non-Solar Energy Sources	0.0810	2.40E-04

Physical Climatology, W.D. Sellers, Univ. of Chicago Press, 1965
 Table 2 on p. 12 is from unpublished notes from
 H.H. Lettau, Dept. of Meteorology, Univ. of Wisconsin.

Earth's Energy Sources

Heat Source	Heat Flux* (W/m ²)	Relative Input
Solar Irradiance	340.25	1.00
Heat Flux from Earth's Interior	0.0612	1.80E-04
Infrared Radiation from the Full Moon	0.0102	3.00E-05
Sun's Radiation Cycle Variability		
Energy Generated by Combustion		
Energy Dissipated in Lightning Discharges	0.0002	6.00E-07
Dissipation of Mechanical Energy of Lightening		
Radiation from Lightening		
Energy of Cosmic Radiation	3.10E-05	9.00E-08
Dissipation of Mechanical Energy of Micrometeorites	2.00E-05	6.00E-08
Total Radiation from Stars	1.40E-05	4.00E-08
Energy Generated by Lunar Tidal Forces in the Atmosphere	1.00E-05	3.00E-08
Radiation from Zodiacal Light	3.40E-06	1.00E-08
Total of All Non-Solar Energy Sources	0.0810	2.40E-04

Solar Cycle Variability makes up about ~ 0.1% of TSI, (~ 10X larger than the second largest energy source)

Temperature on Earth without the Sun would be approximately 30K

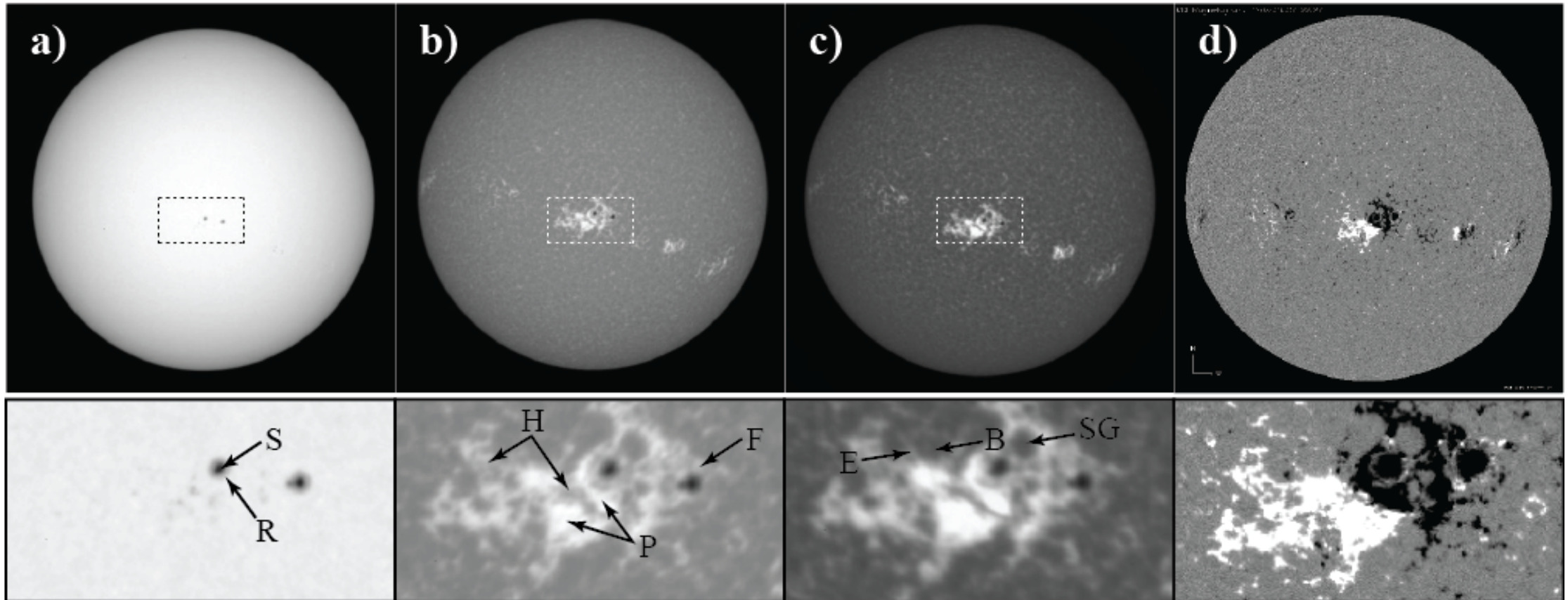
Solar Irradiance Problem

PSPT Red Filter
607.1 nm FWHM= 0.5 nm

PSPT Ca II K
393.4 nm FWHM= 0.3 nm

PSPT Ca II K core
393.4 nm FWHM= 0.1 nm

MDI Magnetogram



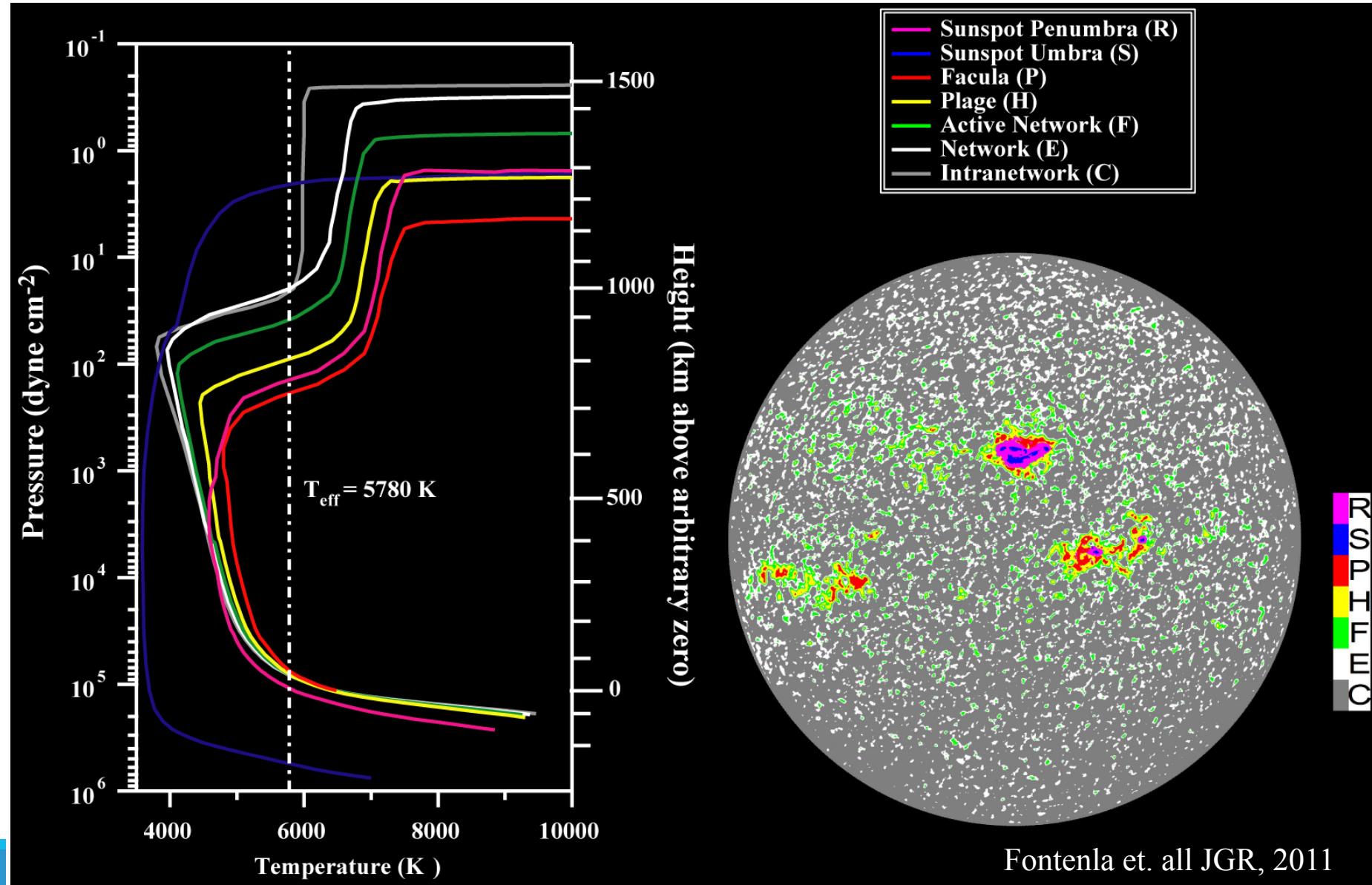
June 7, 2006

SRPM Solar Model

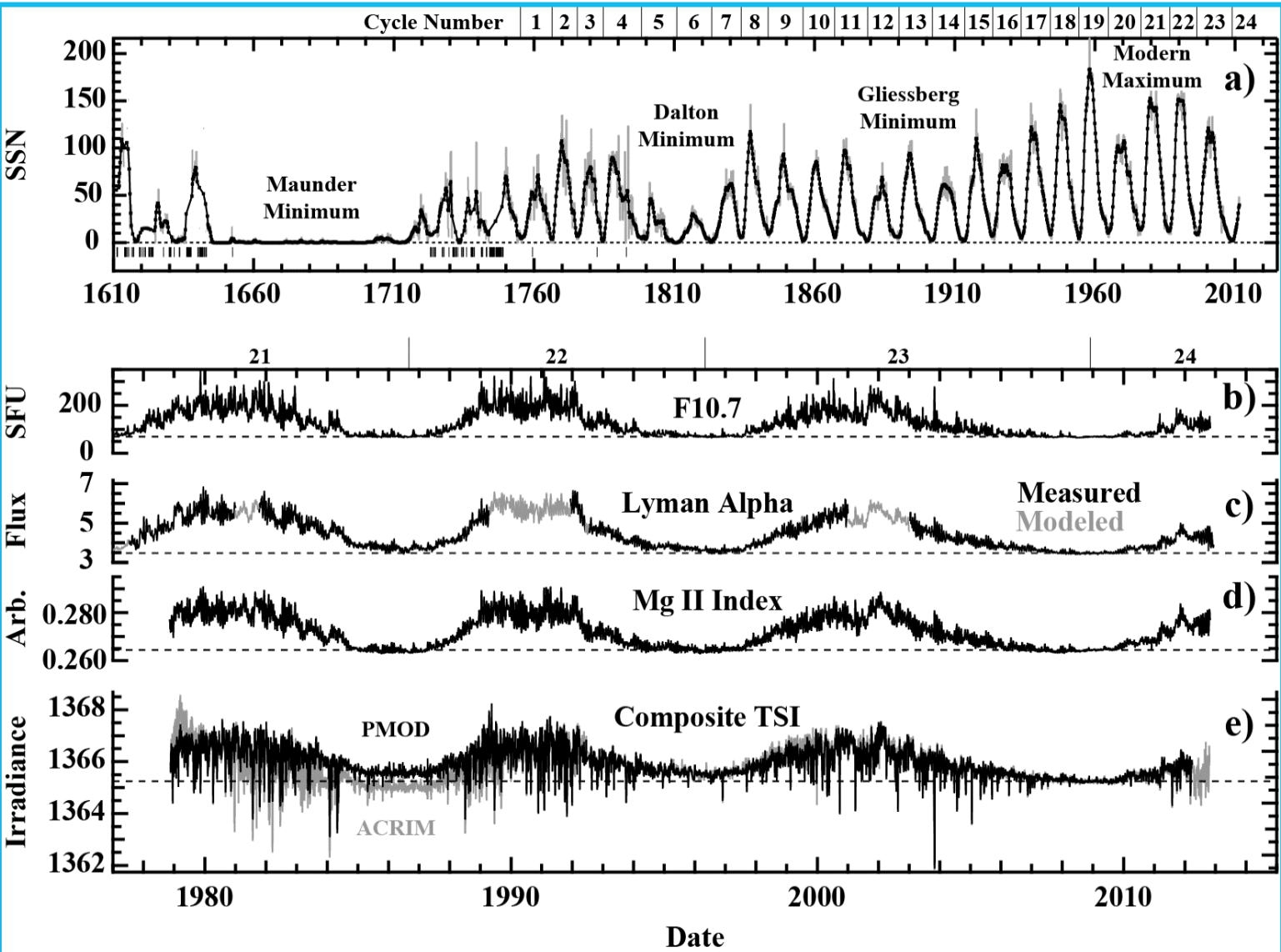
Effective temperature of the Sun found using the Stefan Boltzmann Law

$$T_{\text{effective}} \approx 5780 \text{ K}$$

Each feature of the Sun has a different atmospheric profile



Long Term Records of the Sun



Sun spots record – dates back to the early 17th century, indicative of the overall activity of the photosphere

F10.7 – measured consistently since 1947, originates in the chromosphere and low in the corona

Lyman Alpha – radiates for the entire solar disk, has been measured for the past 40 years

Mg II Index – correlates well with the EUV in the upper atmosphere of the Sun, measurements began around 1980



PSPT Instrumentation

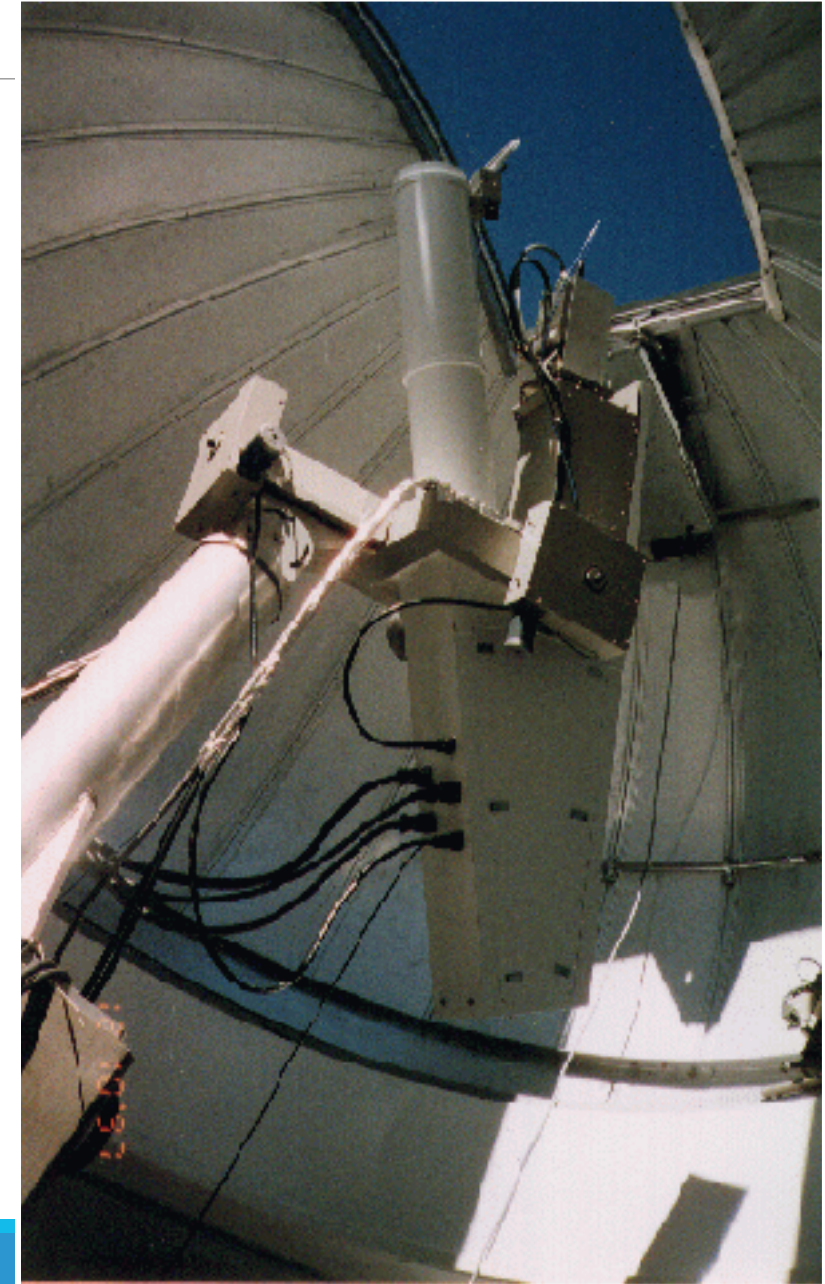
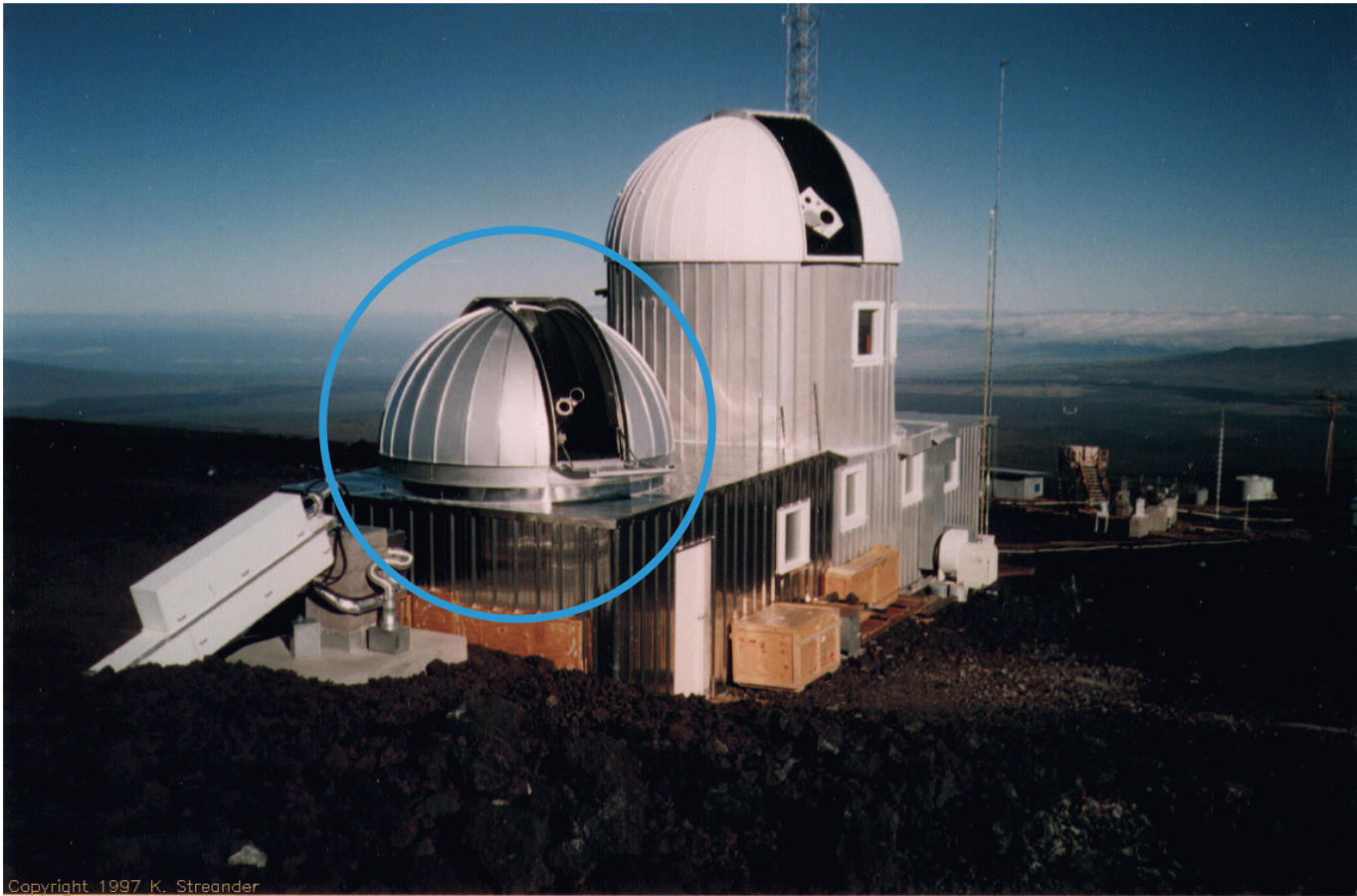
SECTION 2

PSPT Basics

PSPT – Precision Solar Photometric Telescope

Located at the Mauna Loa Solar Observatory

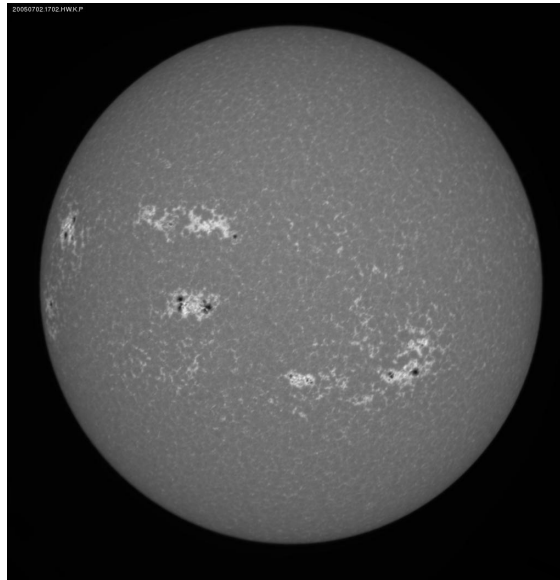
- Ideal due to the clean site, less atmospheric interference, etc.



Targeting Different Layers of the Sun through Images

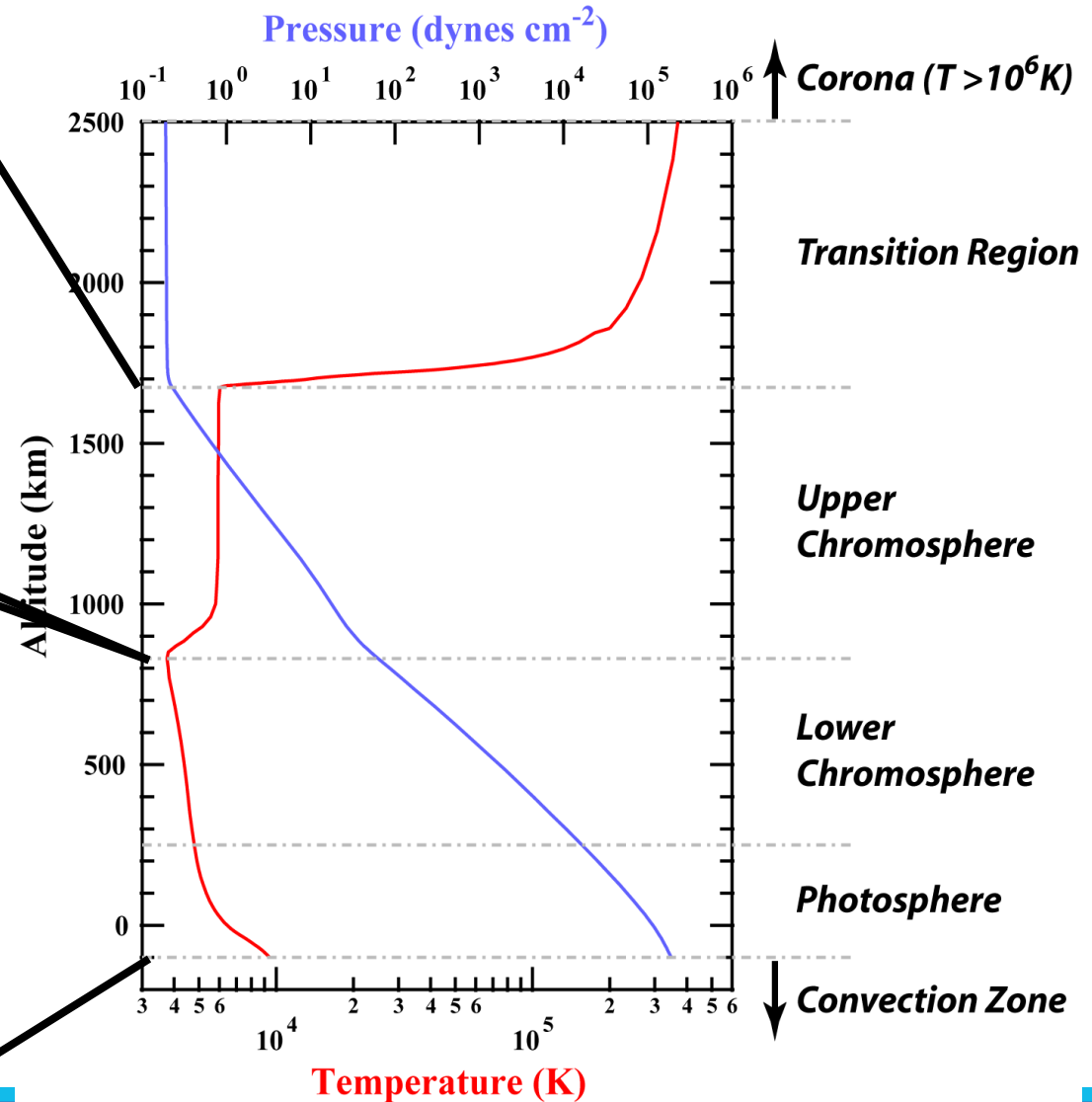
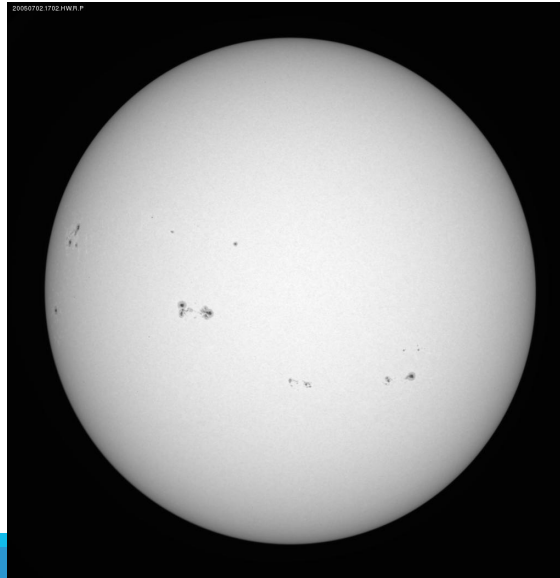
Calcium II Image:

- Shows bright regions in the upper chromosphere
- Facula, plage, active network, etc.



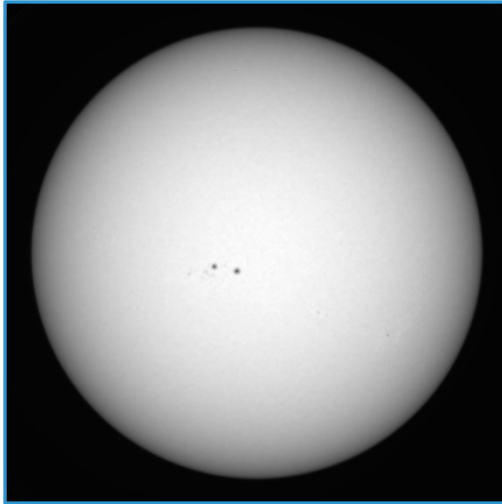
Red Image:

- Shows darker regions, biased towards the lower chromosphere and photosphere
- Sunspots – umbra and penumbra

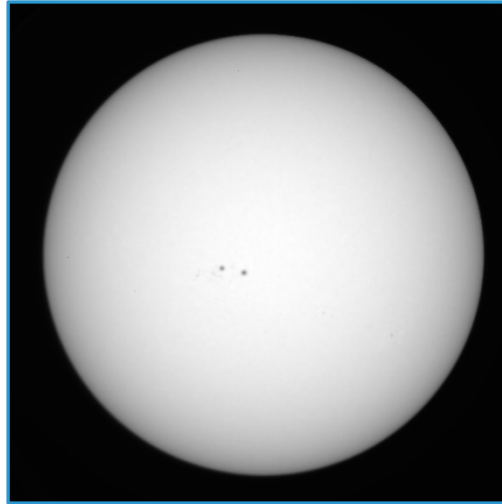


Sample Images from PSPT

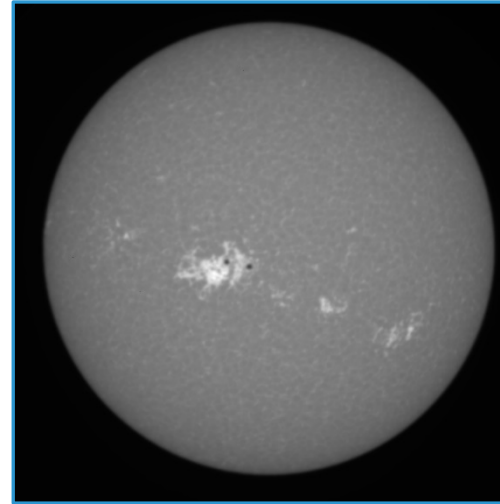
Blue (409.4 nm)



Red (607.1 nm)

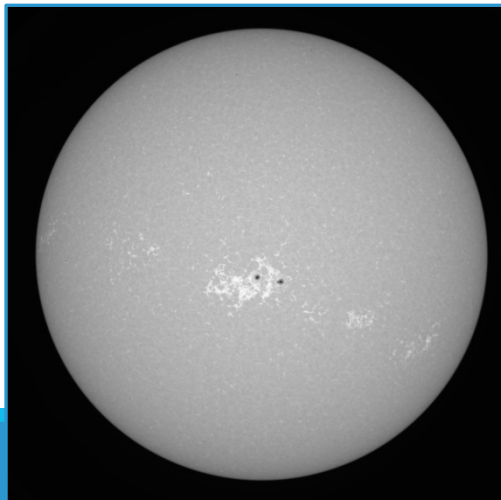


Ca II K (393.4 nm)

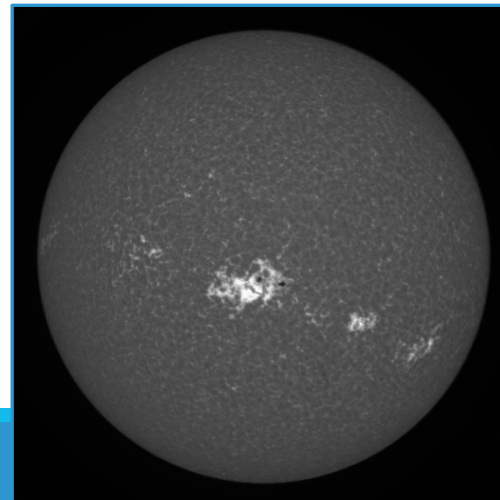


**Each image taken by the PSPT is
2048x2048**

Ca II K NBW (393.6 nm)



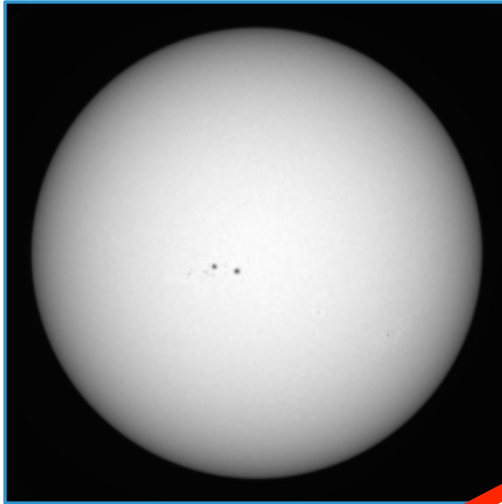
Ca II K NBC (393.4 nm)



**PSPT features 0.1% pixel-to-
pixel relative photometric
precision**

Sample Images from PSPT

Blue (409.4 nm)



Red (607.1 nm)



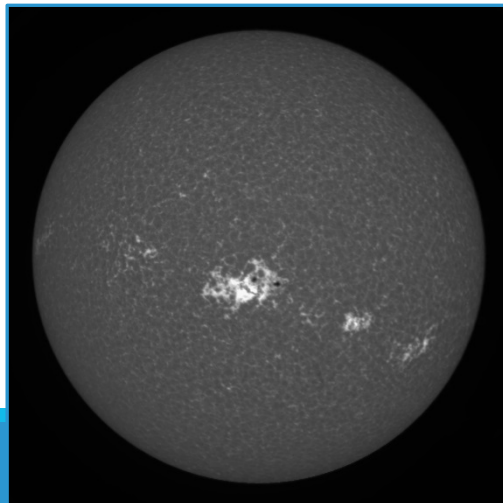
Ca II K (393.4 nm)



Each image taken by the PSPT is 2048x2048

PSPT features 0.1% pixel-to-pixel relative photometric precision

Ca II K NBC (393.4 nm)



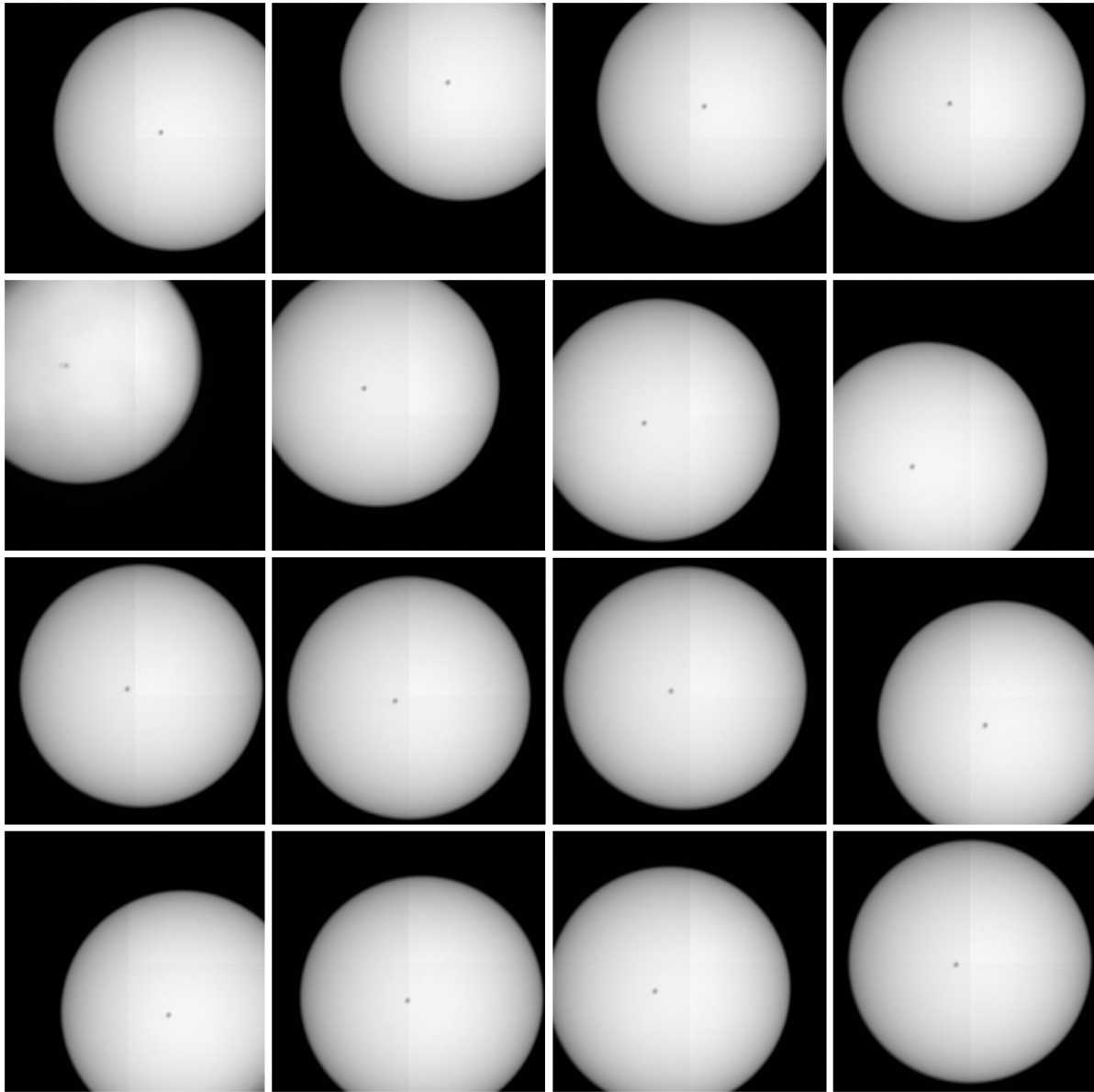
Finished Product Images

Image Flat-Fielding

SECTION 3



What is Flat-Fielding?



**Method based on Lin and Kuhn (1991)
Algorithm**

**Instrument calibration using a set of 16
images**

PSPT makes this calibration once a day

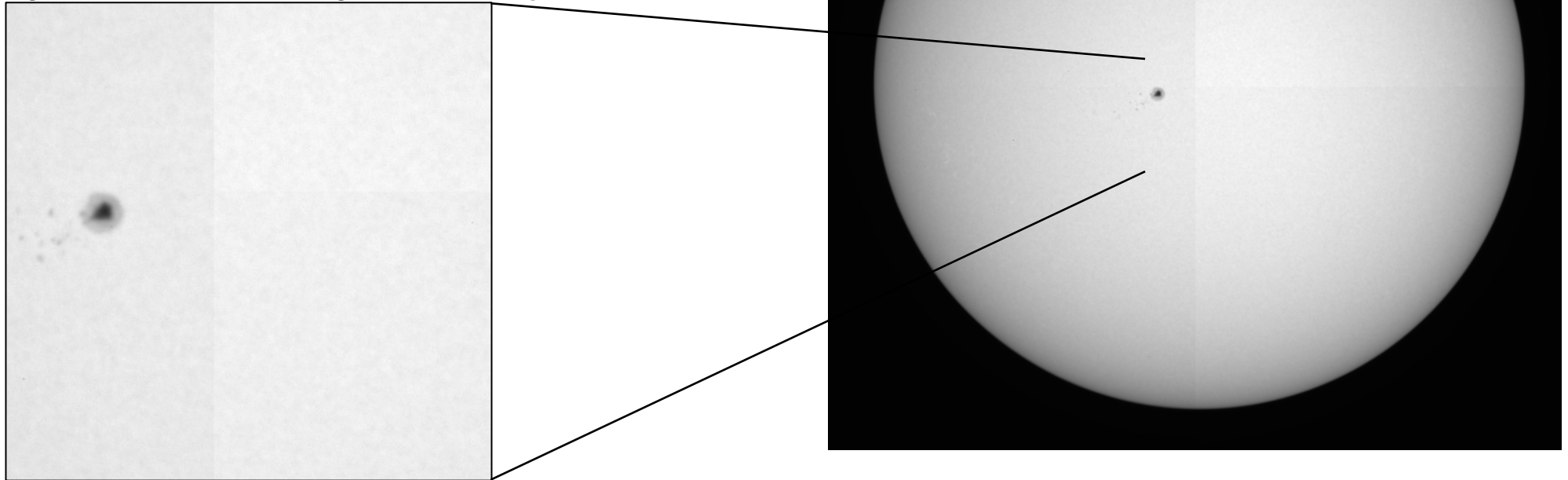
**Distinguish instrument artifacts from solar
details**

The Kuhn-Lin Method

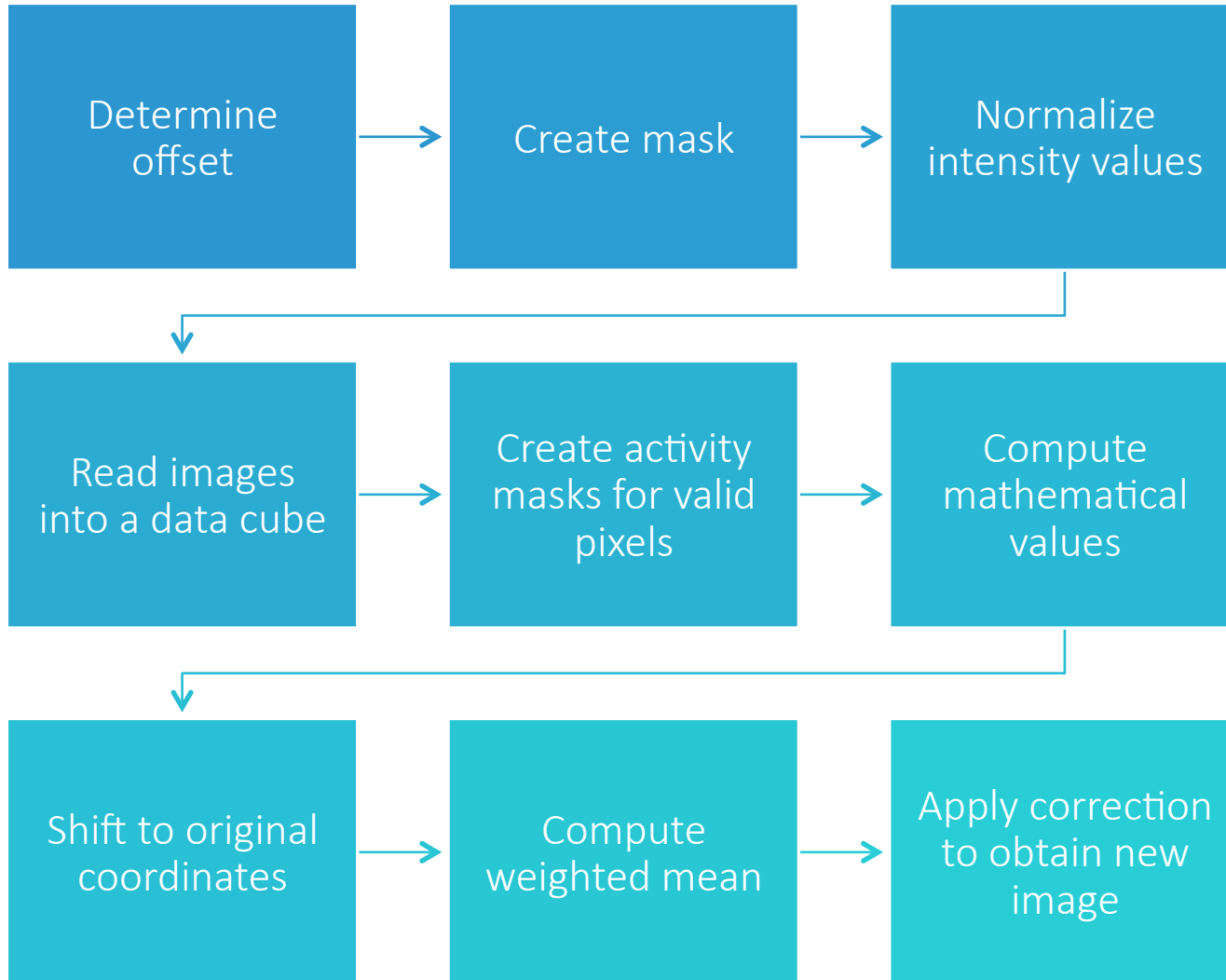
Accuracy up to 0.10% is required

Performs the calibration in the telescope's operating environment

- Not only does it remove the instrument's defects but also the environmental offset (temperature, atmosphere, etc)



Algorithm



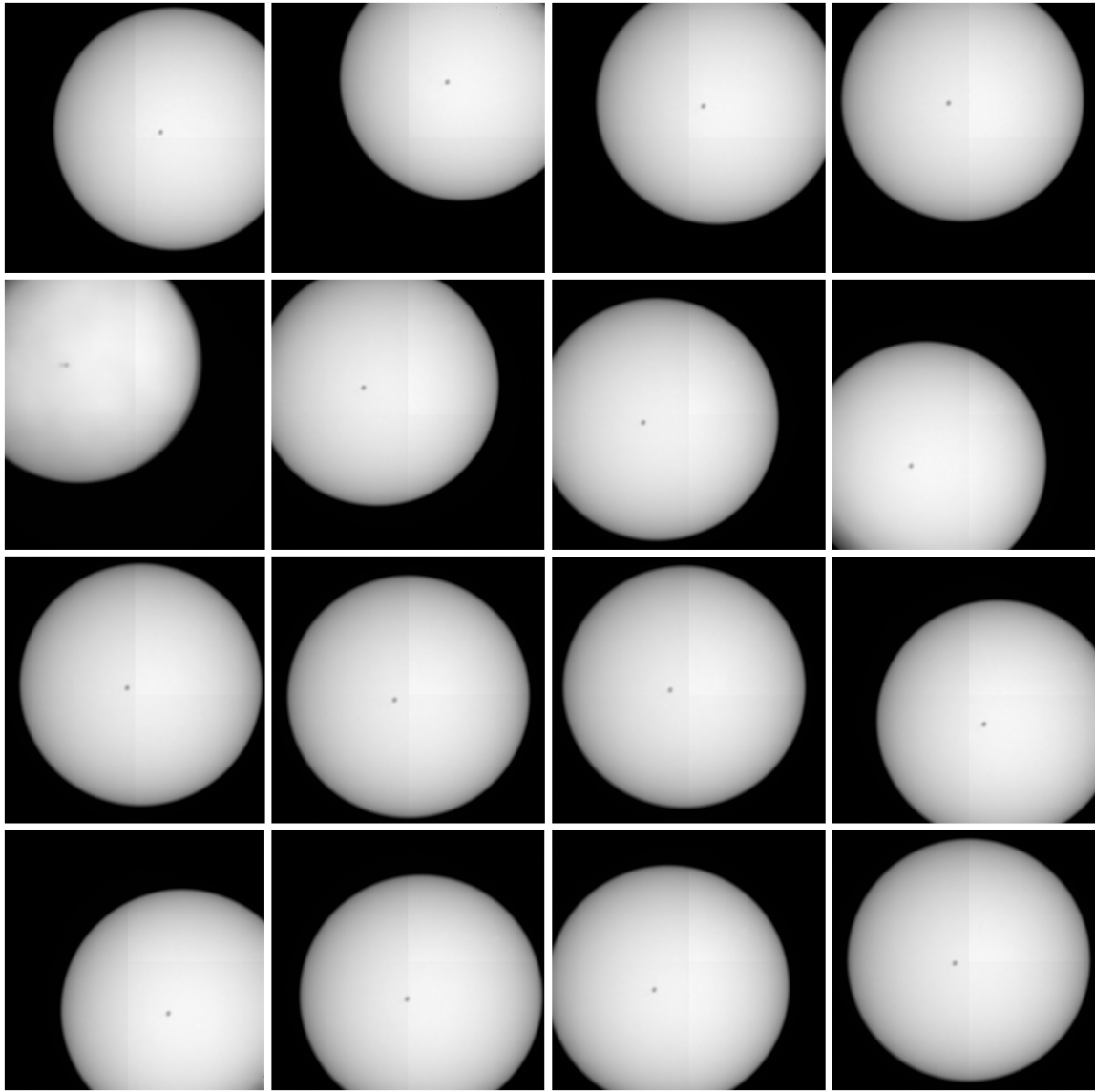
Processing this code takes quite a while

- Mathematically intensive
- Large data sets

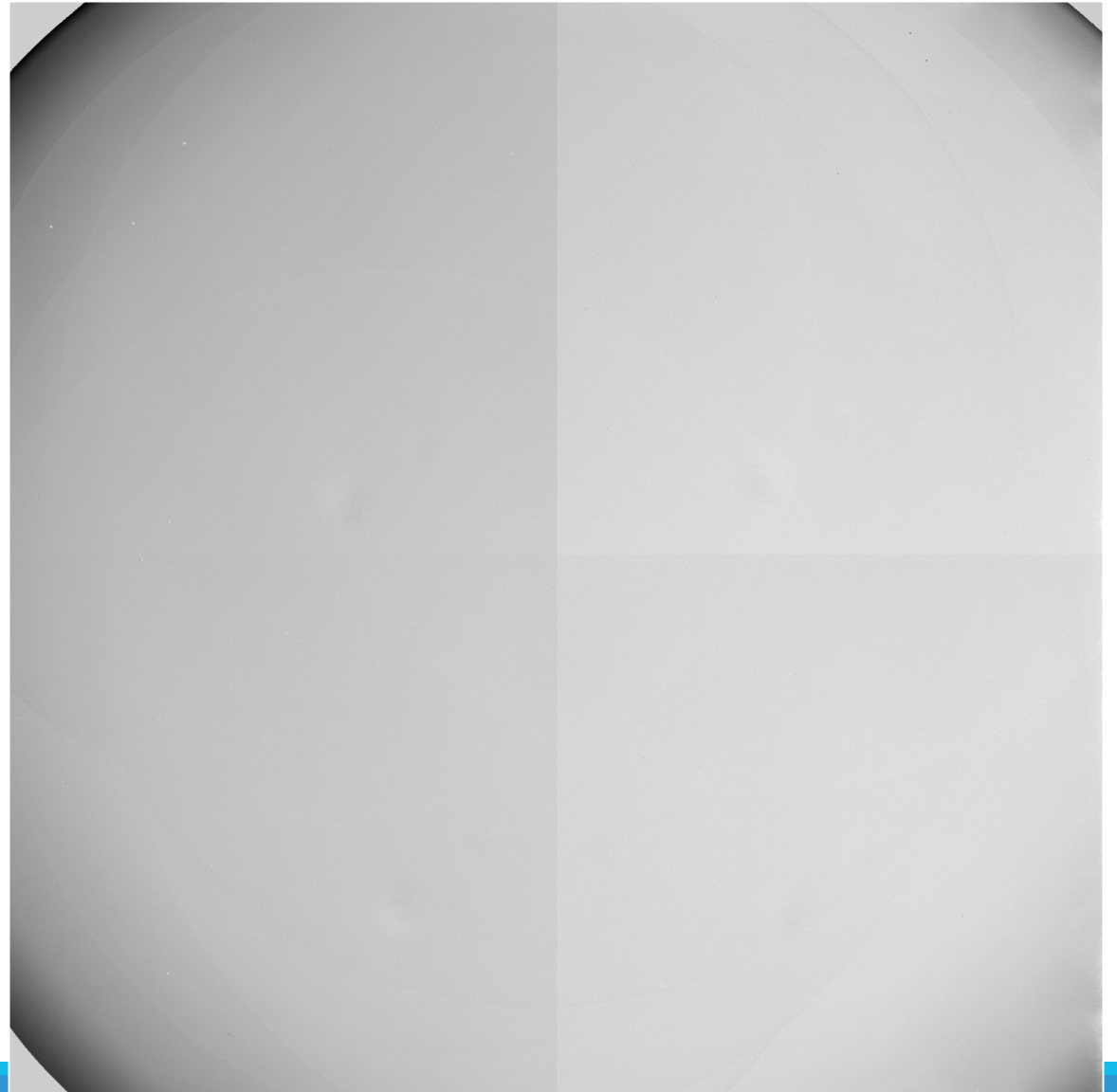
Repeated until stopping criteria is met

- Standard deviation $< 10^{-6}$
- Could take up to 40 iterations

Offset Images to Flat Field

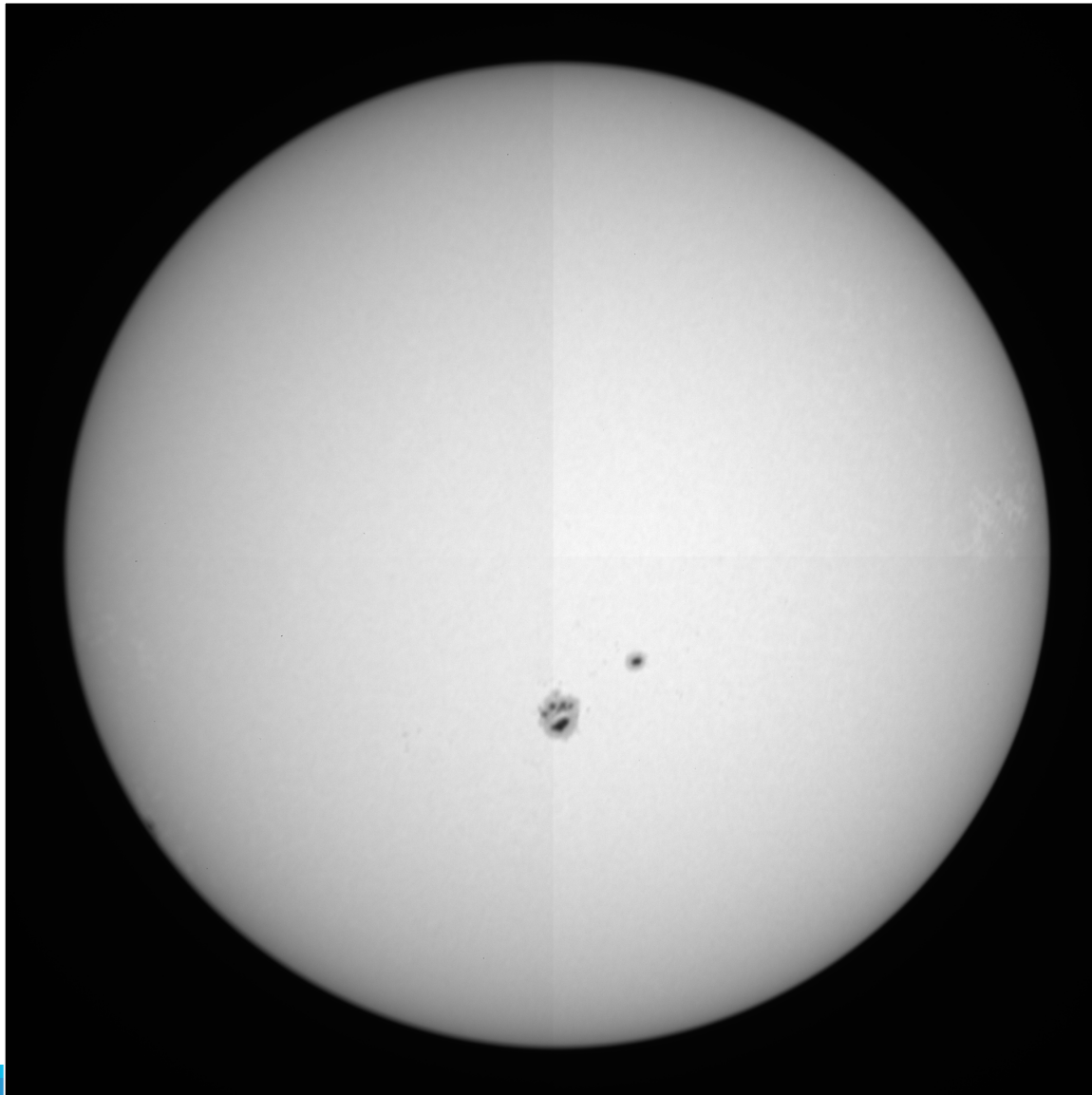


16 Offset Images

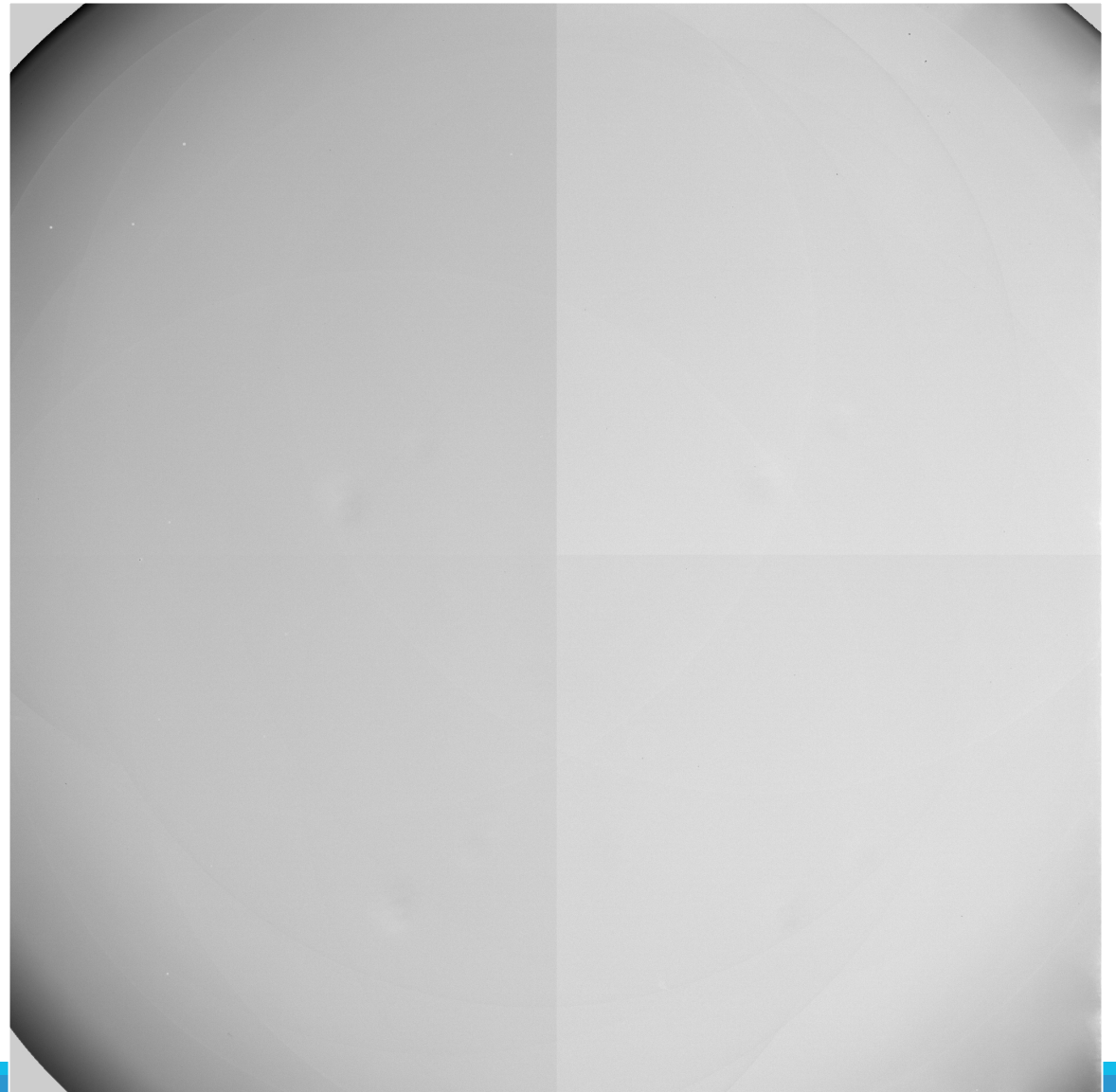


Generated Flat Field

Original Image Divided by Flat Field

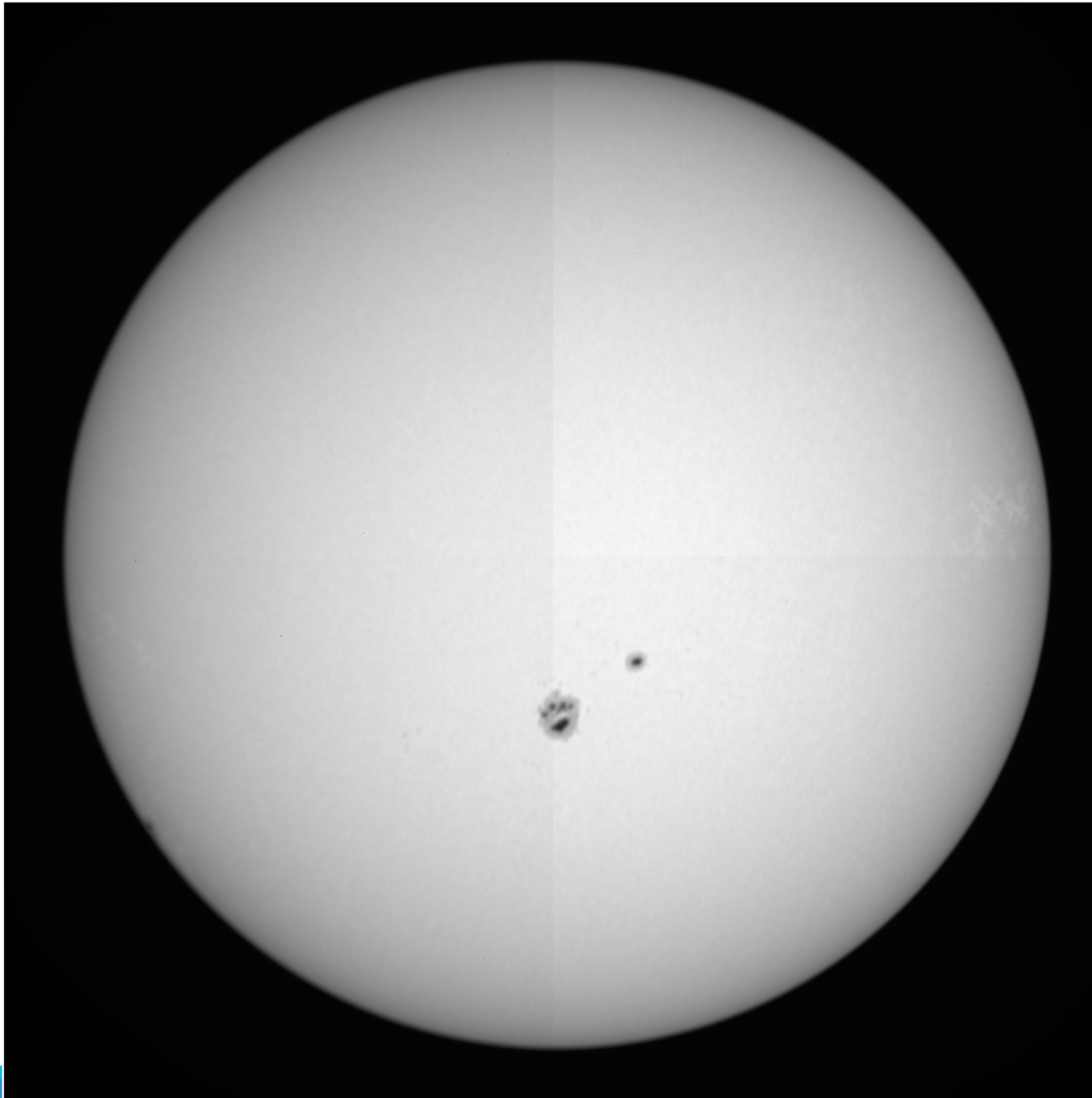


Raw Image

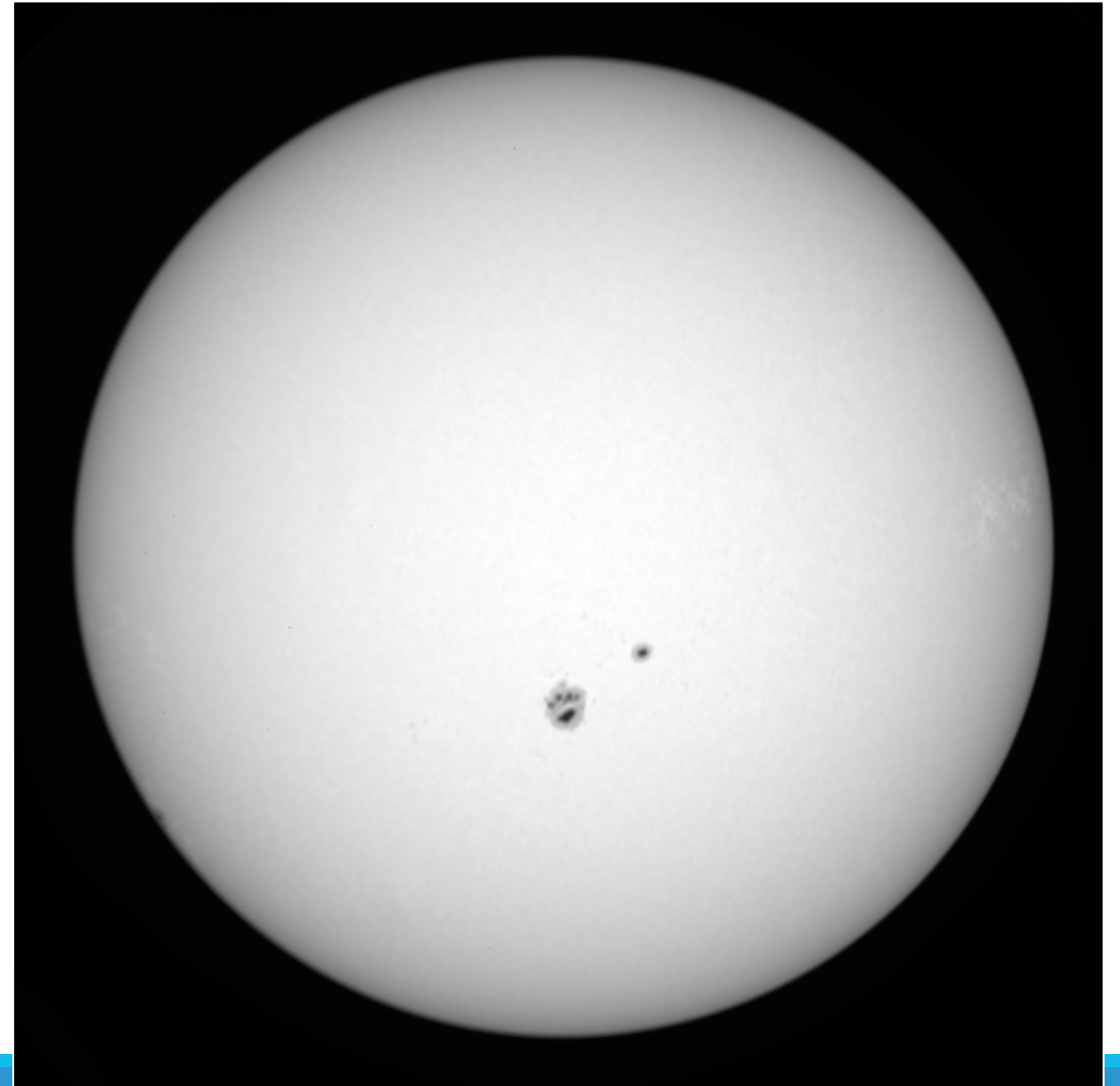


Generated Flat Field

Final Image with Removed Artifacts

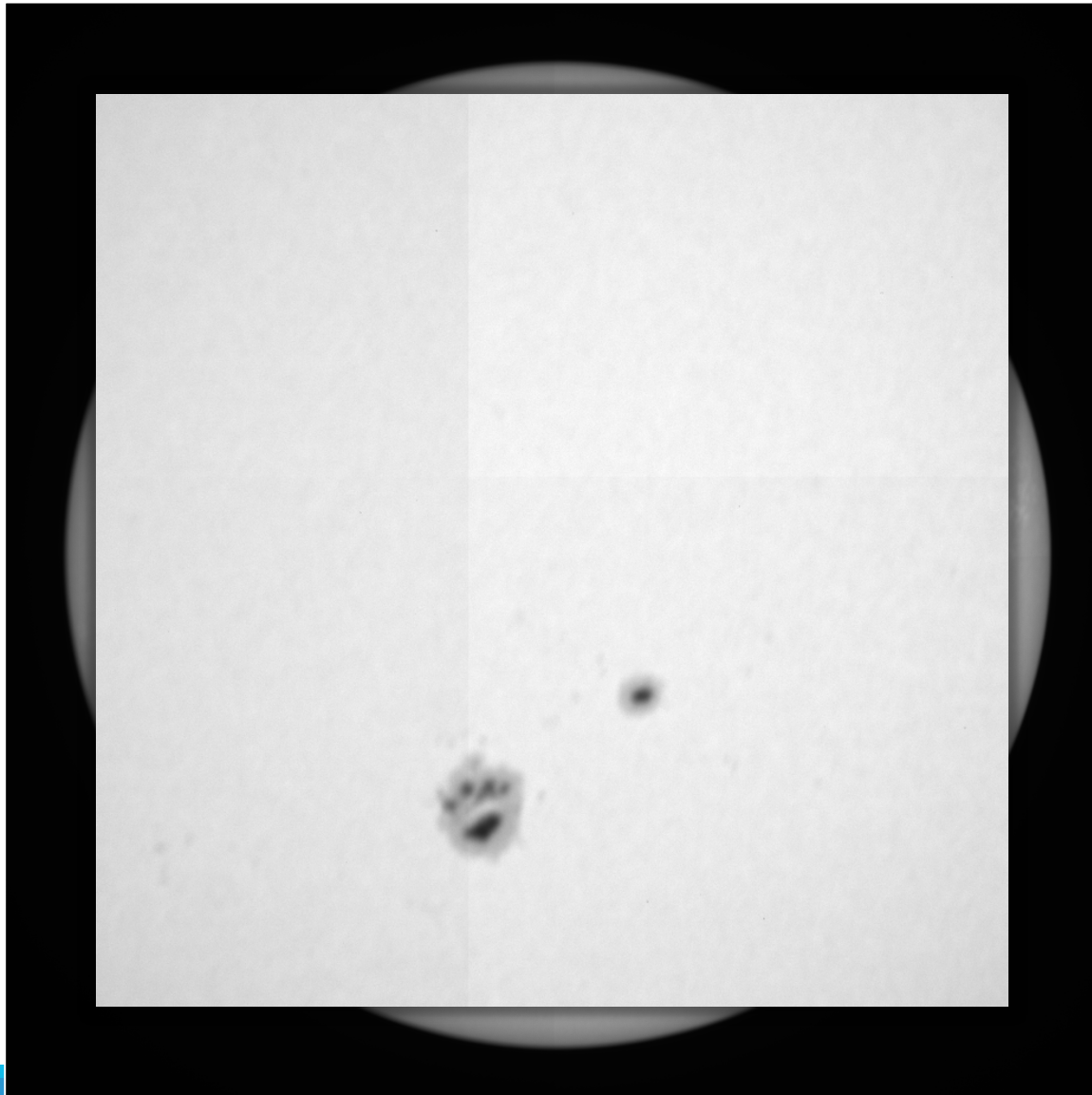


Raw Image

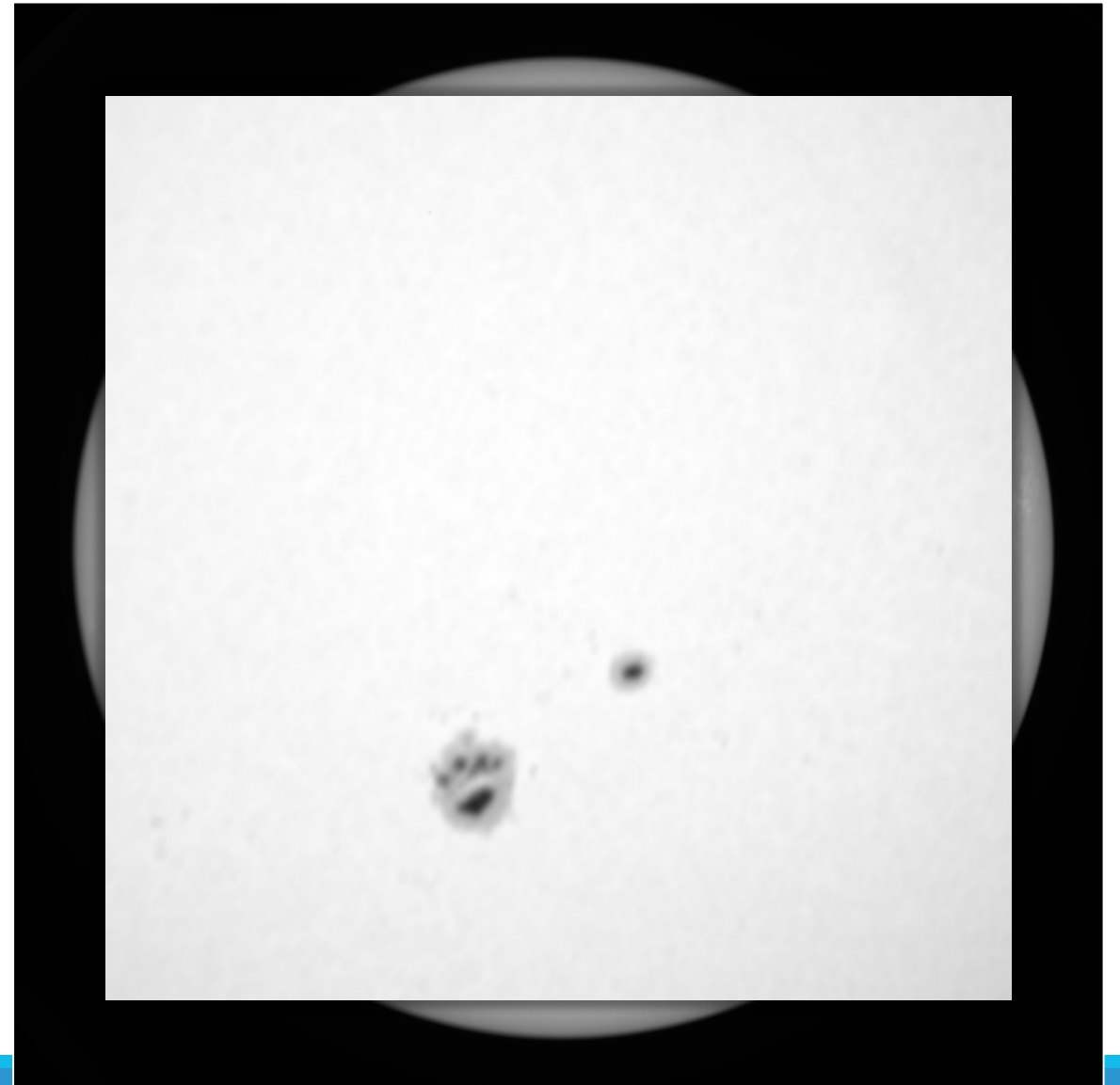


Final Image

Final Image with Removed Artifacts



Raw Image



Final Image

Summary of Flat Field Analysis

Execution time

- Original code was written in IDL and required about 24 hours to produce a flat field
 - IDL and Python are interpretive languages – meaning efficiency is sacrificed
- Code implemented in C++ compiled under Portland Group Compiler (PGCC) reduced time to around 20 minutes
 - C++ and Fortran much more efficient with memory allocation
- Therefore, moving to CUDA (parallel processing language) would allow the most efficient use of memory
 - Allocates memory as threads that are executable concurrently

However, CUDA is unable to read the current data cubes that are stored in the code – instead they need to be translated to “threads” and “blocks” that are native to parallel processing code

- Currently existing code does not support this kind of process

The solution is feasible, but a fundamental rewrite of the operation of the functions inside the flat-fielding code is needed

- This is a very valuable activity but it needs practices suitable to parallel processing

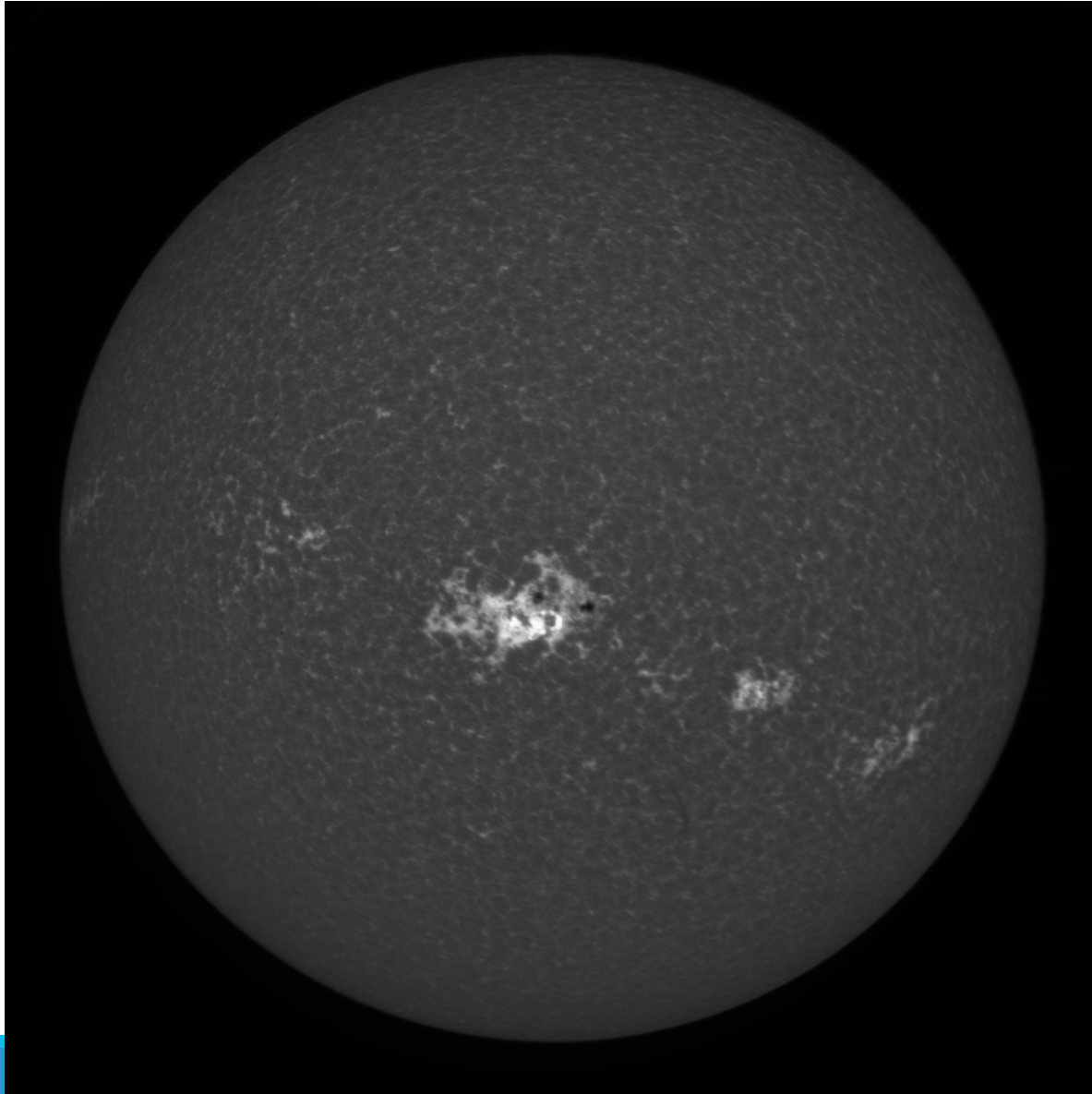


Core-to-Wing Imaging in Ca

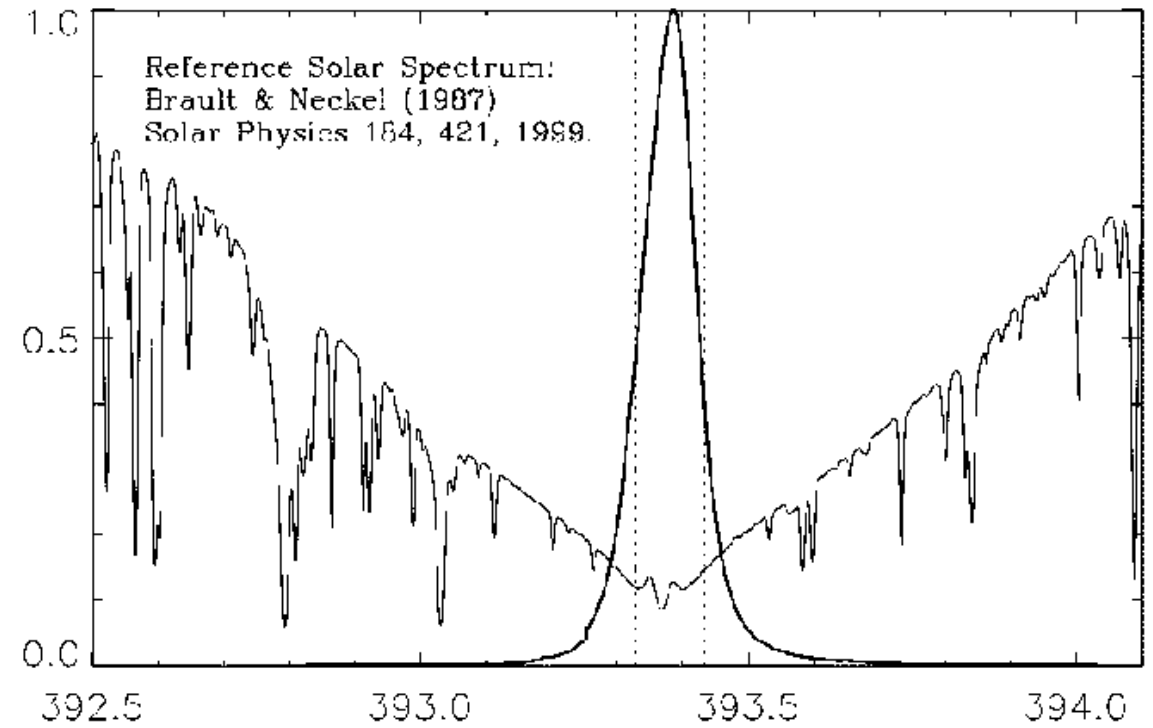
II

SECTION 4

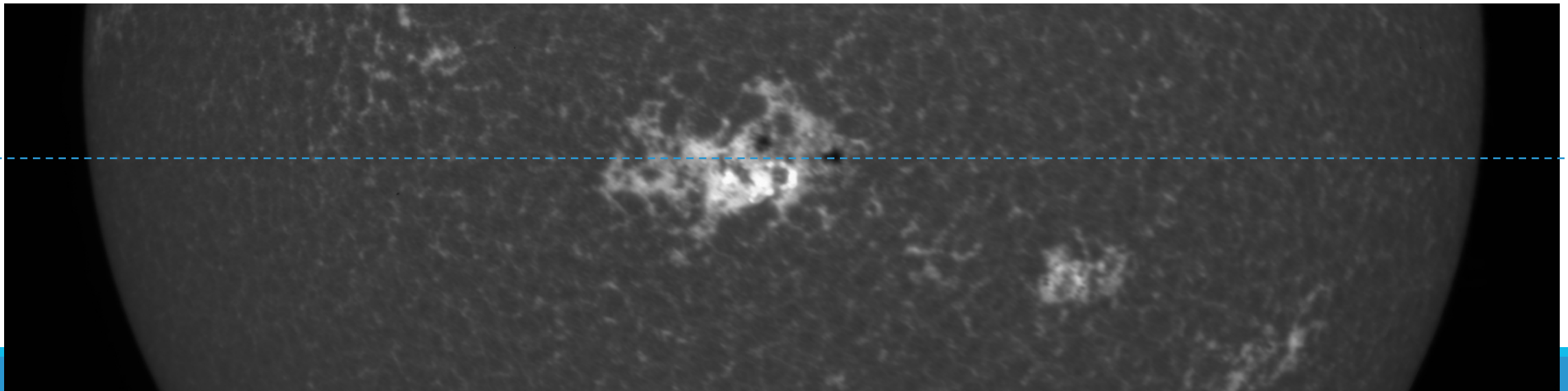
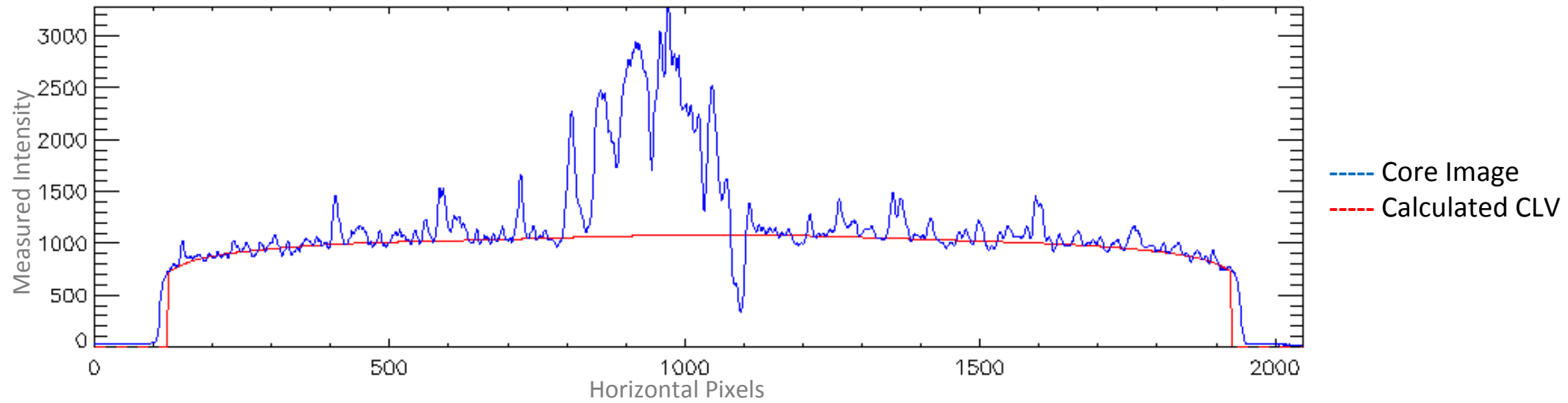
Calcium II Core



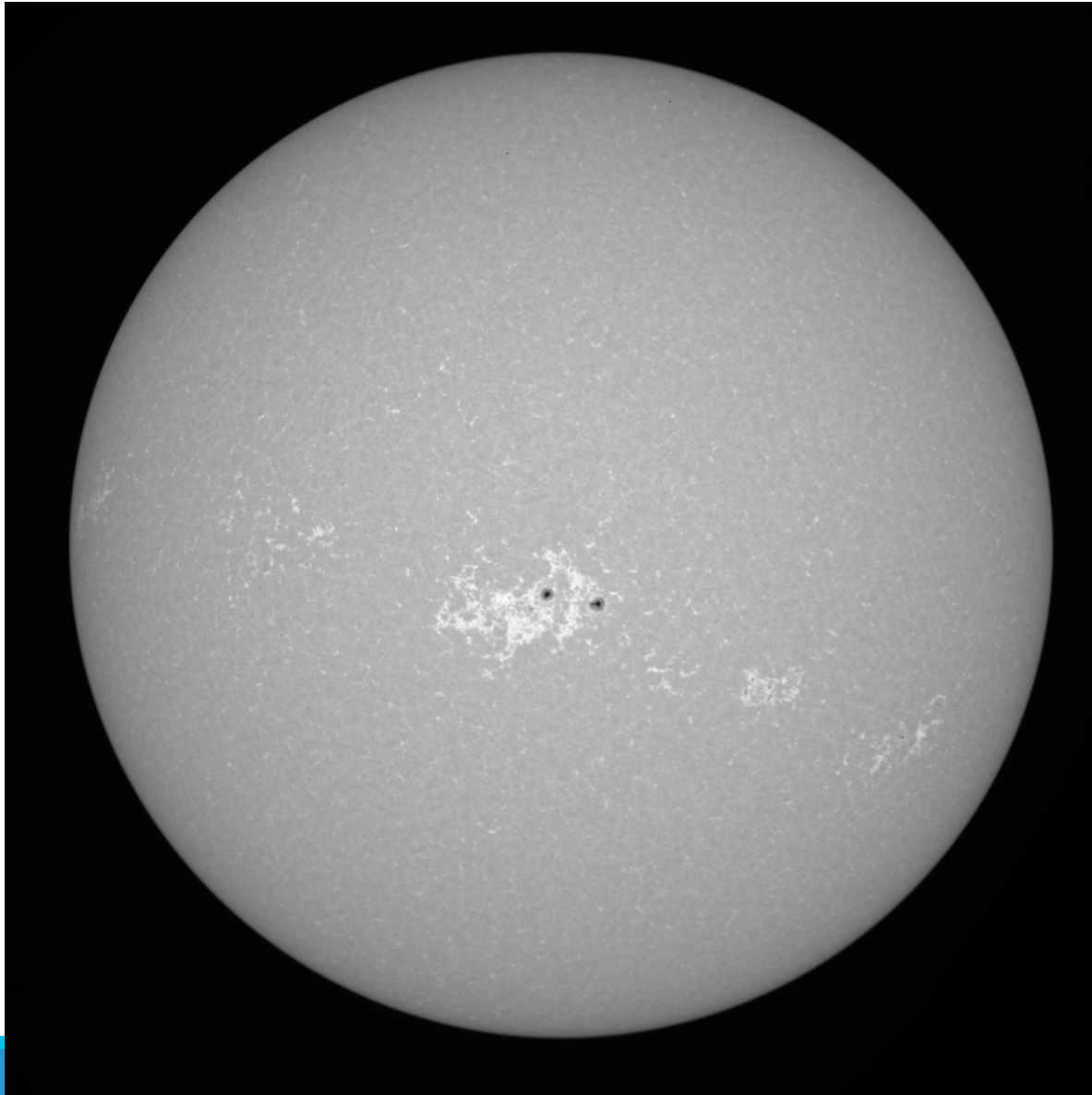
CaIIK Narrow Center: 393.379nm
FWHM: 0.103nm



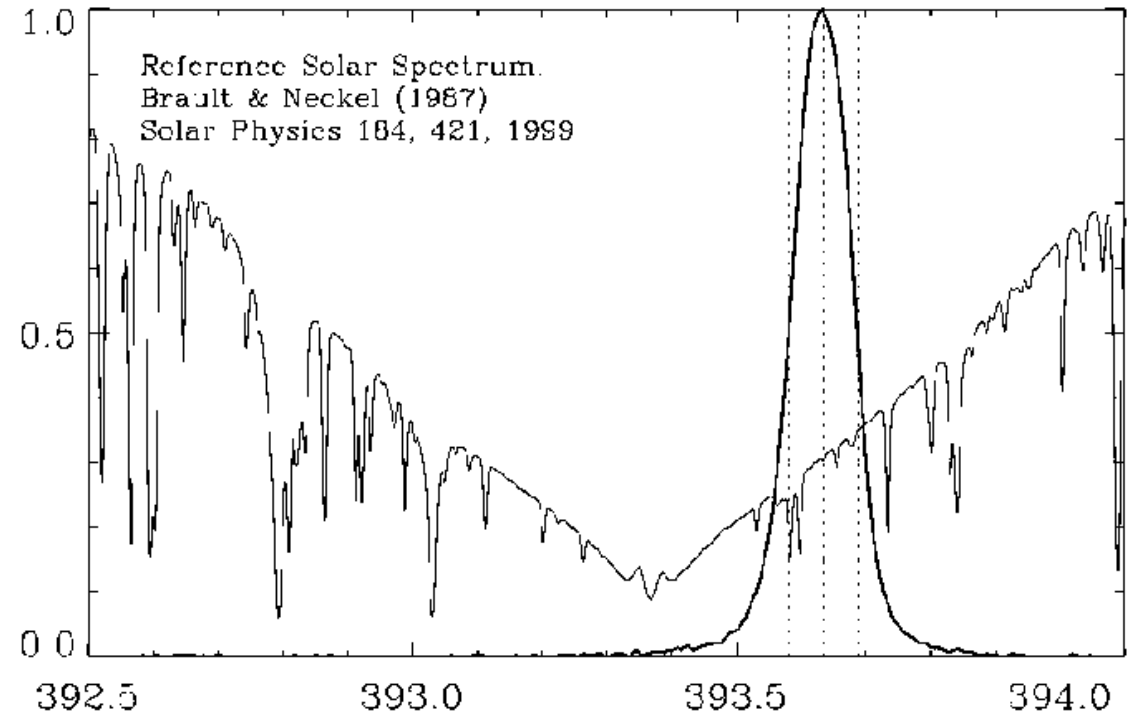
CLV for Calcium II Core



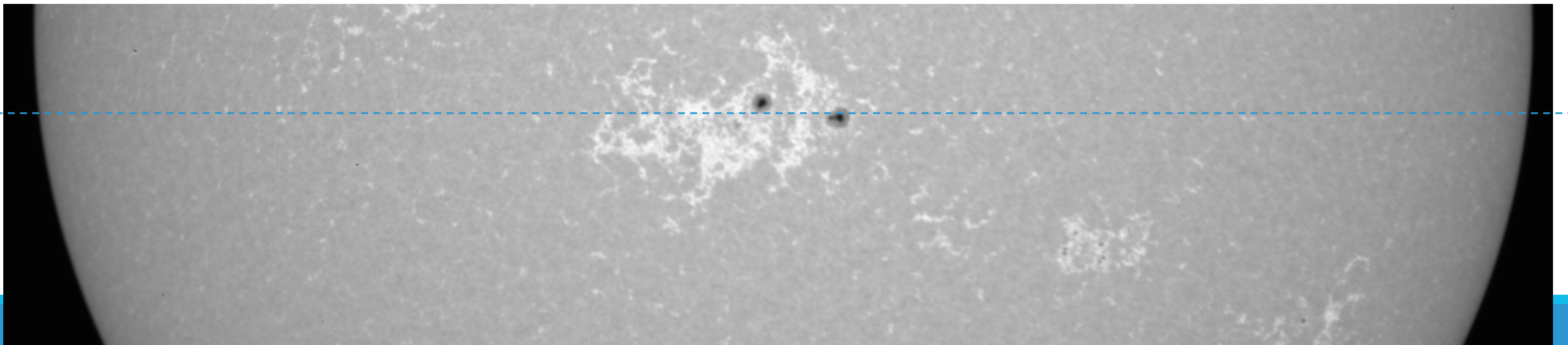
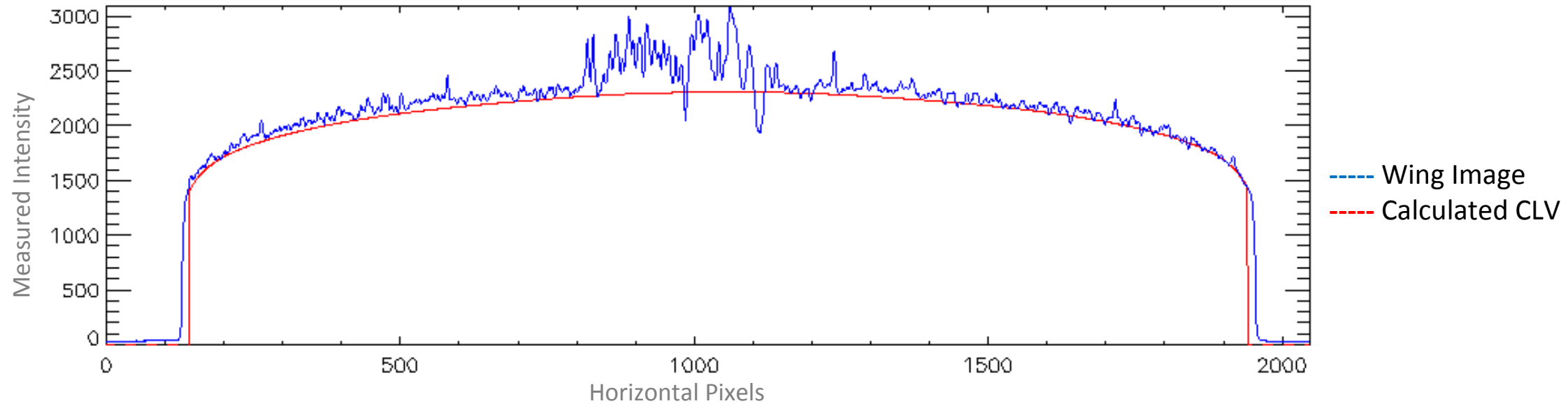
Calcium II Wing



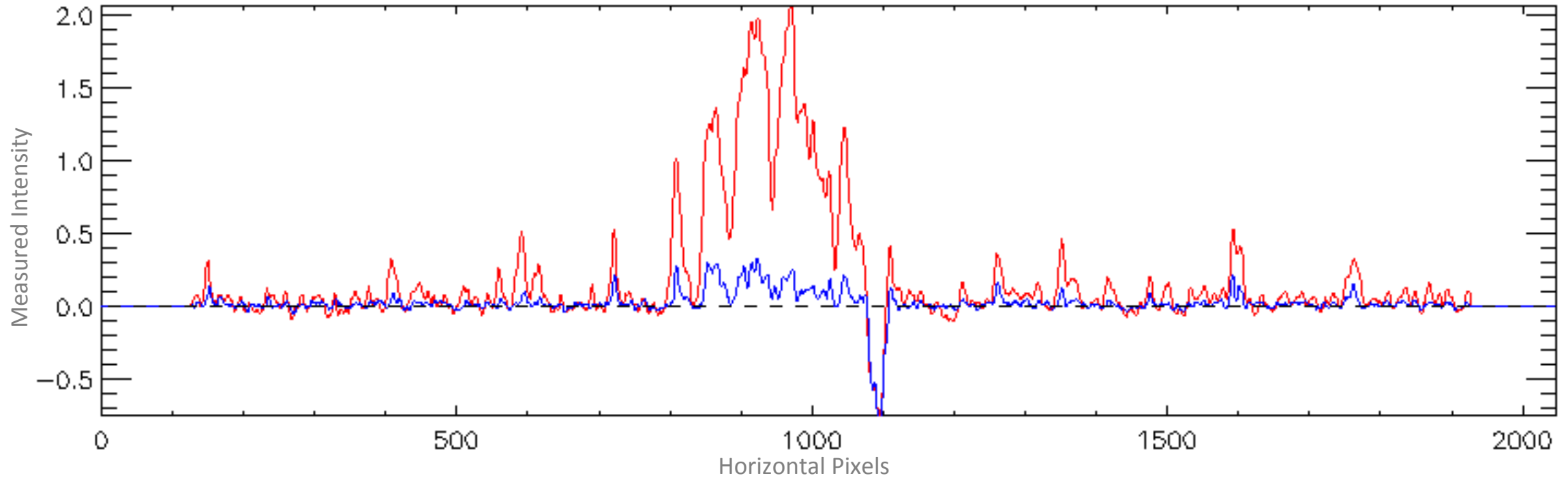
CaIIK Narrow Wing: 393.634nm
FWHM: 0.106nm



CLV for Calcium II Wing



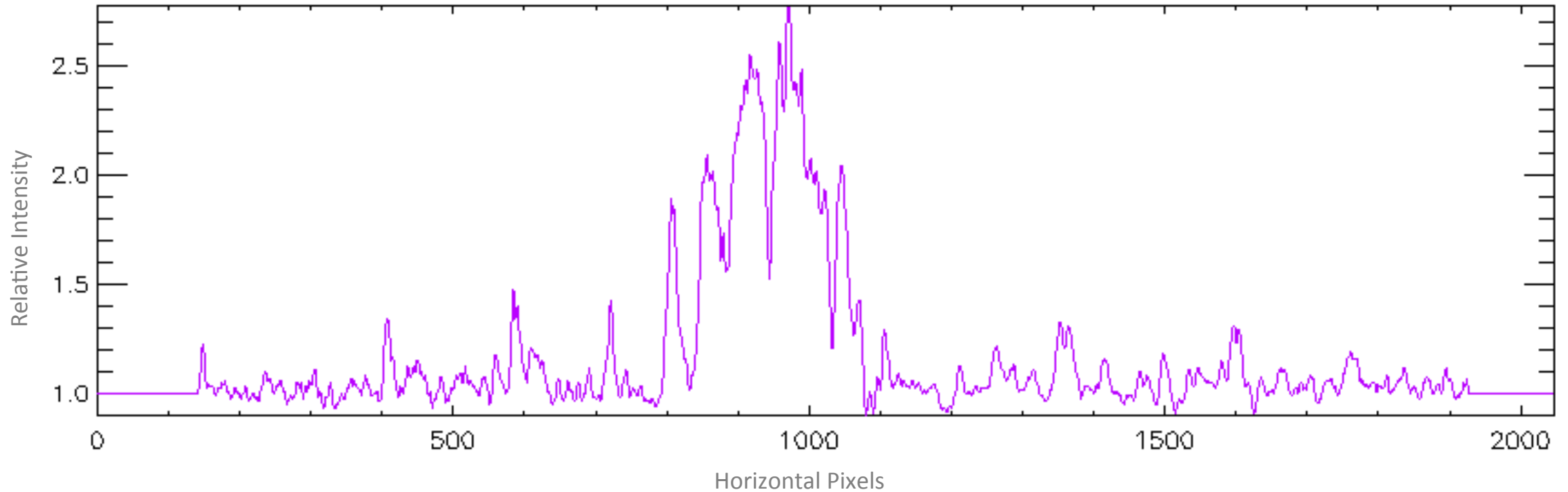
Core-to-Wing Ratio Slice



Core Contrast = Core Image / Core CLV

Wing Contrast = Wing Image / Wing CLV

Core-to-Wing Ratio Slice

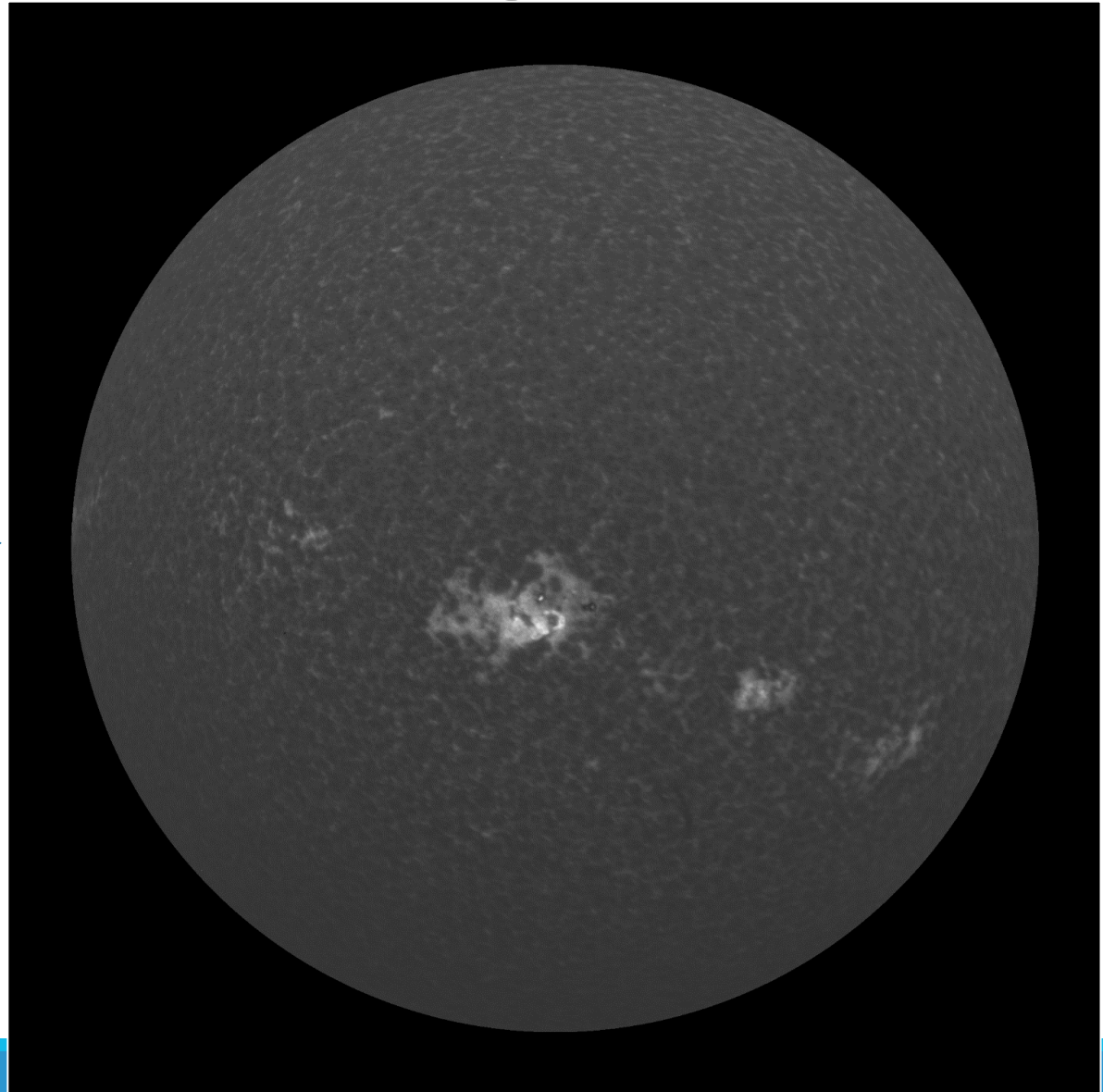
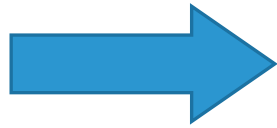
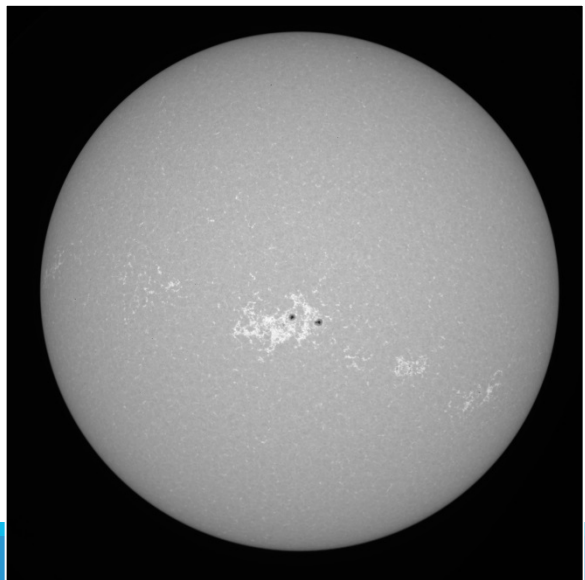
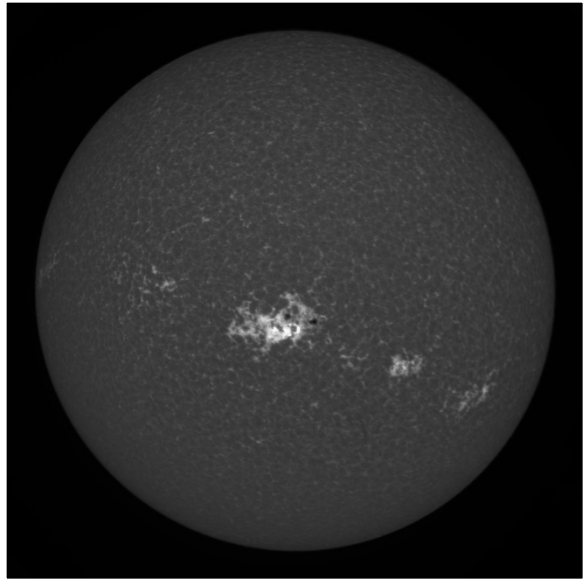


Core Contrast = Core Image / Core CLV

Wing Contrast = Wing Image / Wing CLV

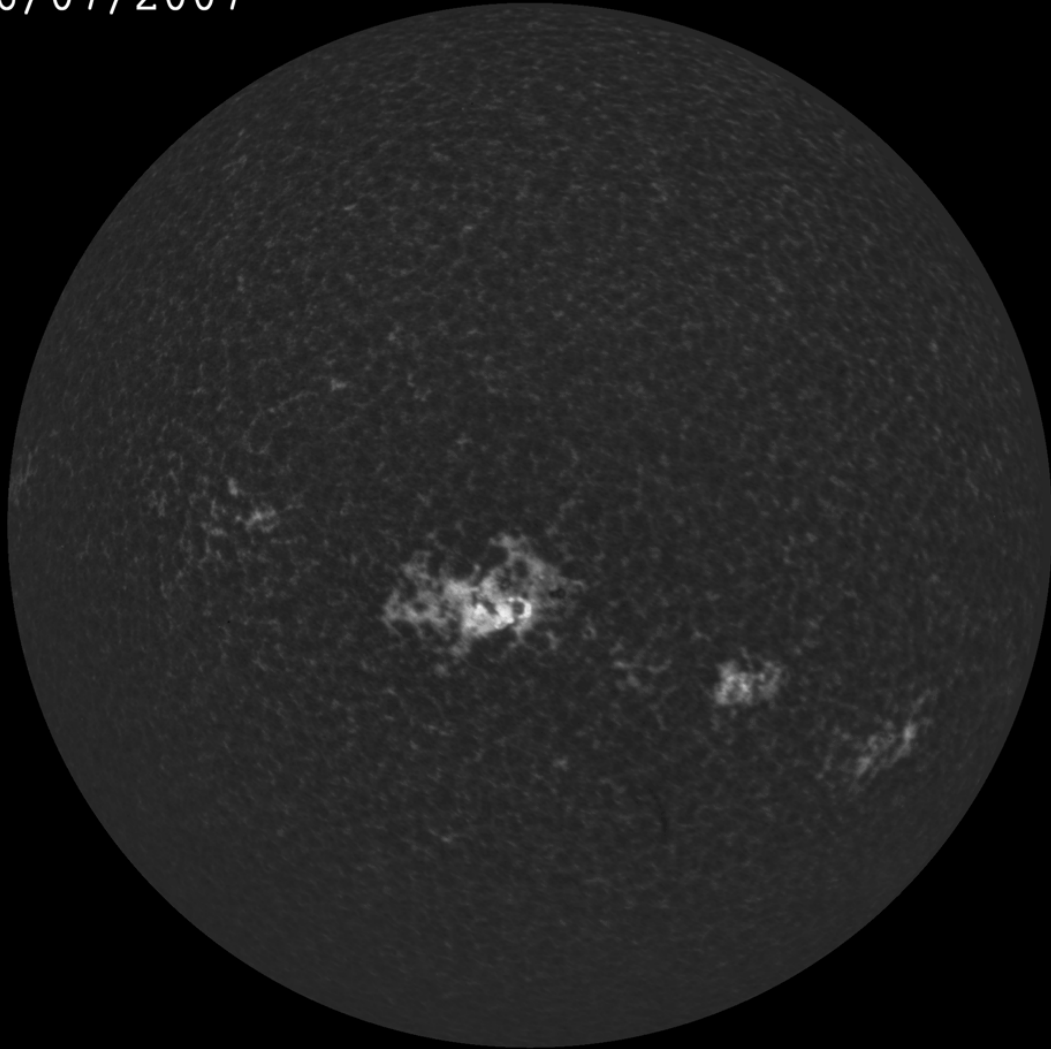
Core to Wing Image = Core Contrast / Wing Contrast

Core-to-Wing Ratio Image



Core-to-Wing Ratio Image

06/07/2007



June 6th, 2007 to July 8th, 2007

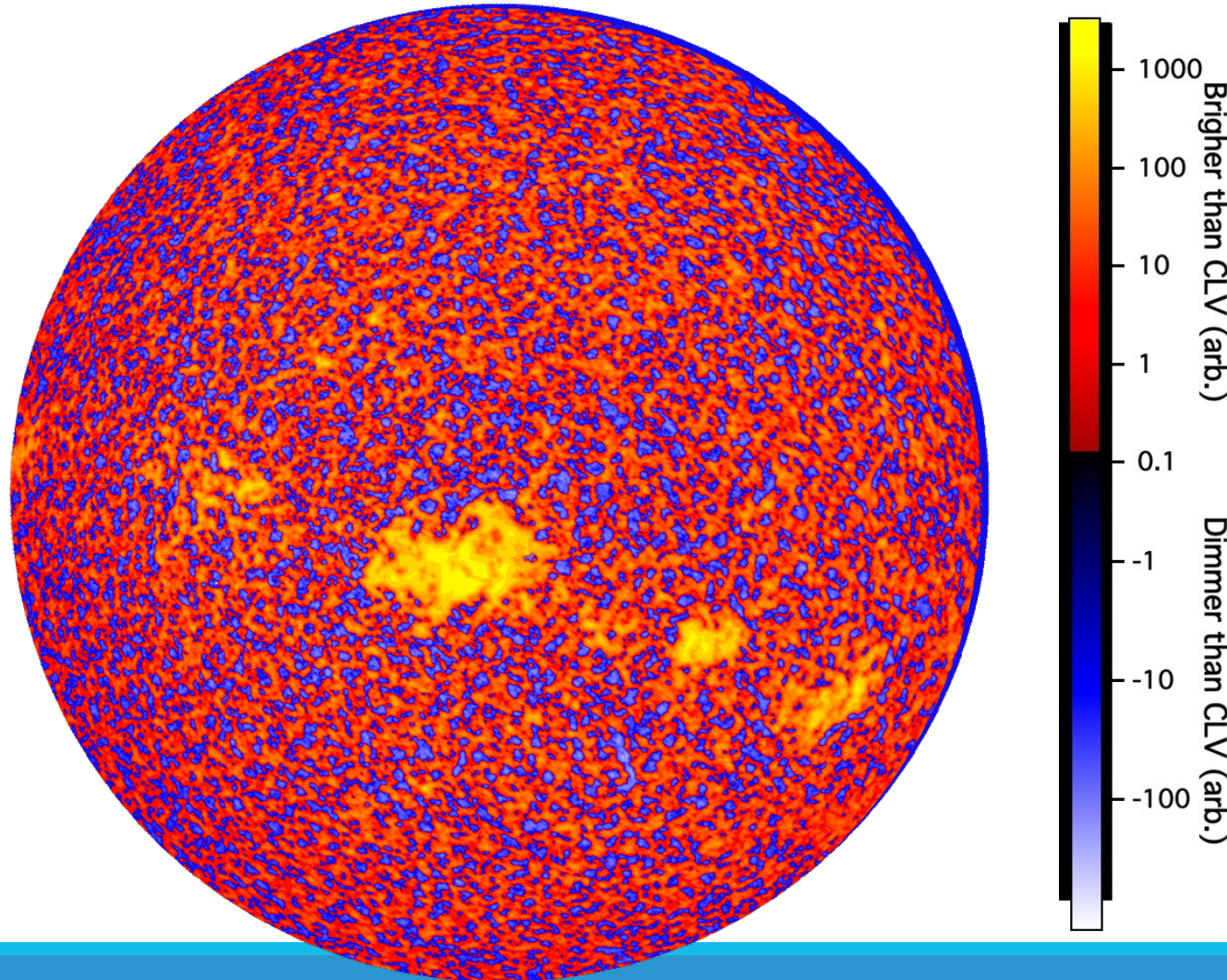
- Period of low solar activity
- Solar minimum was two years away

Image shows intensity linearly

Allows easier viewing of brighter regions of the Sun

CLV Comparison

06/07/2007



June 6th, 2007 to July 2nd, 2007

Intensity is drawn on out a logarithmic scale to better see the variation

Typically network $\sim 4x$ greater than the plage and facula

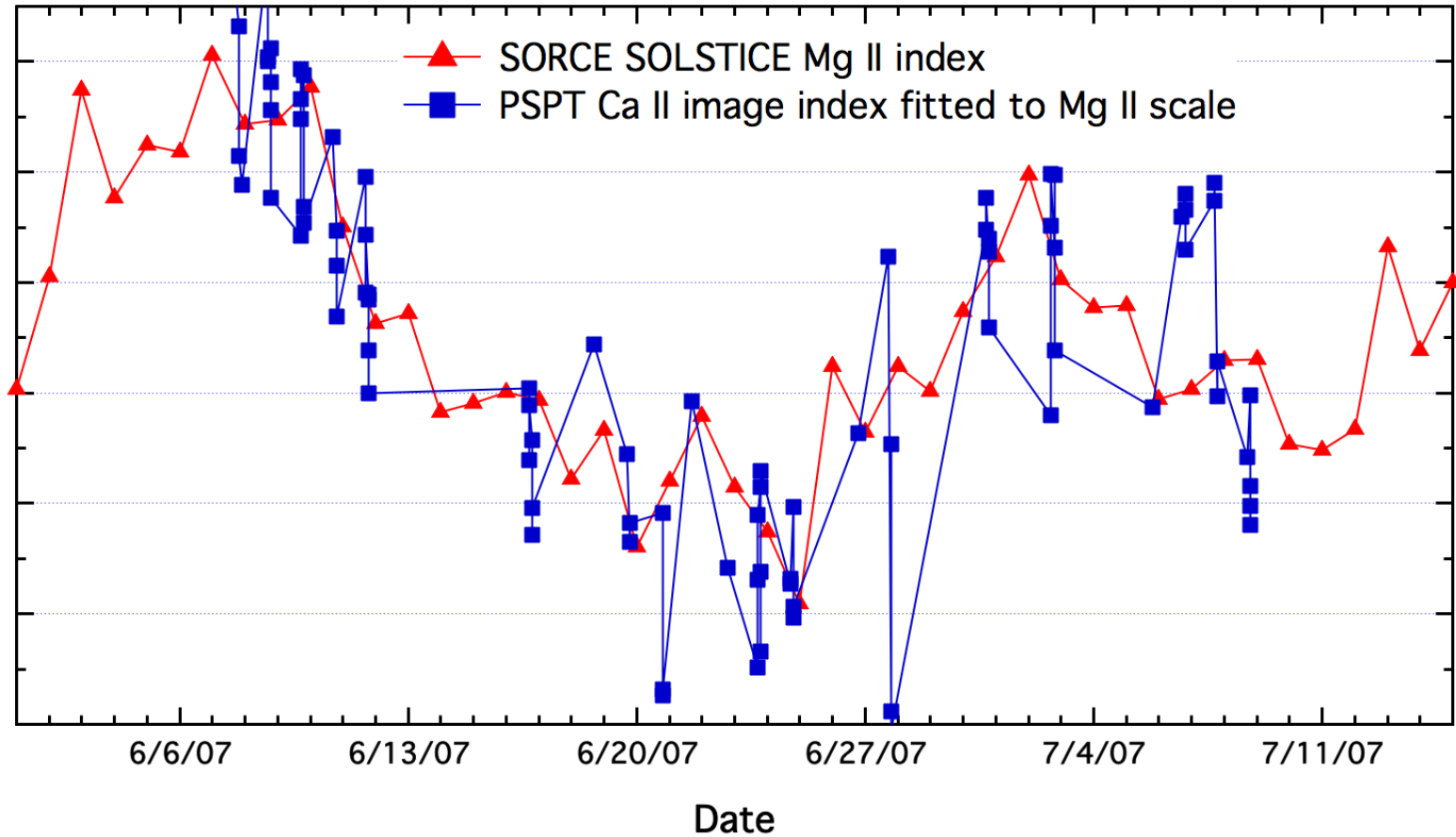
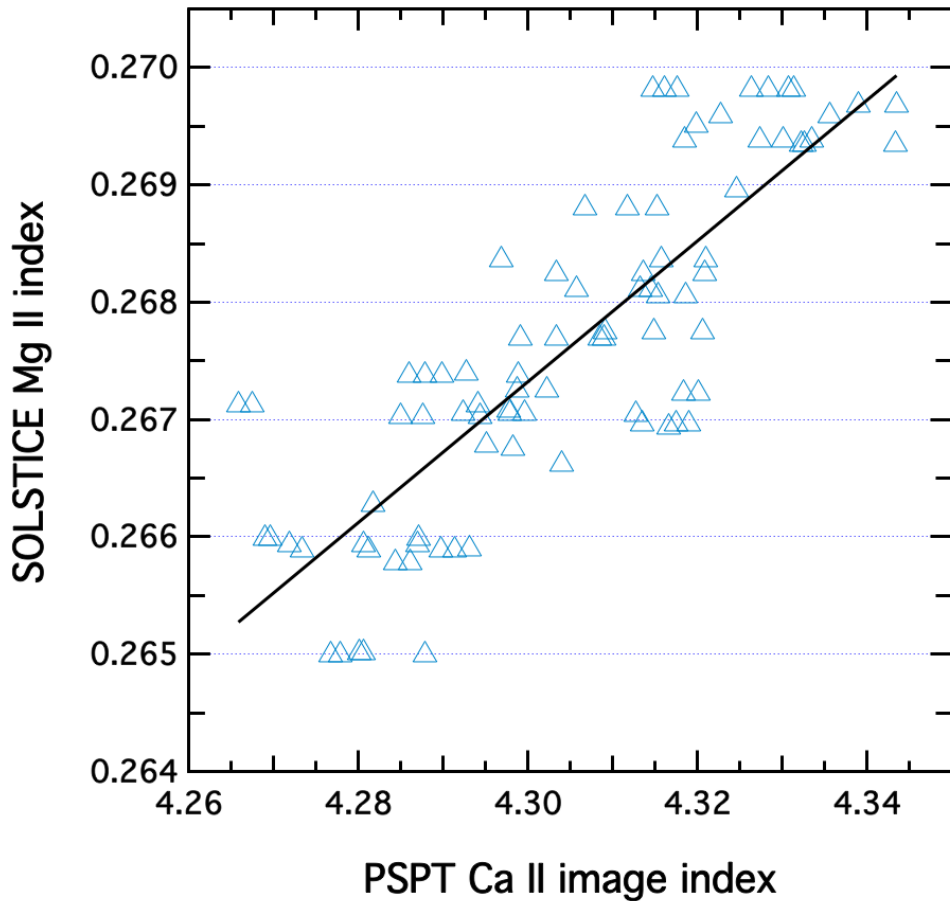
Smaller variations in network could become comparable to contributions from facula and plage

Ca II vs. Mg II Data

$$\text{Mg II Index} = (0.0093 \pm 0.038) + (0.060 \pm 0.009) * \text{Ca II image Index}$$

$r^2 = 0.686$; 95% confidence interval

$$\text{Ca II image index} = \sum \text{Ca CW pixels} / 10^6$$



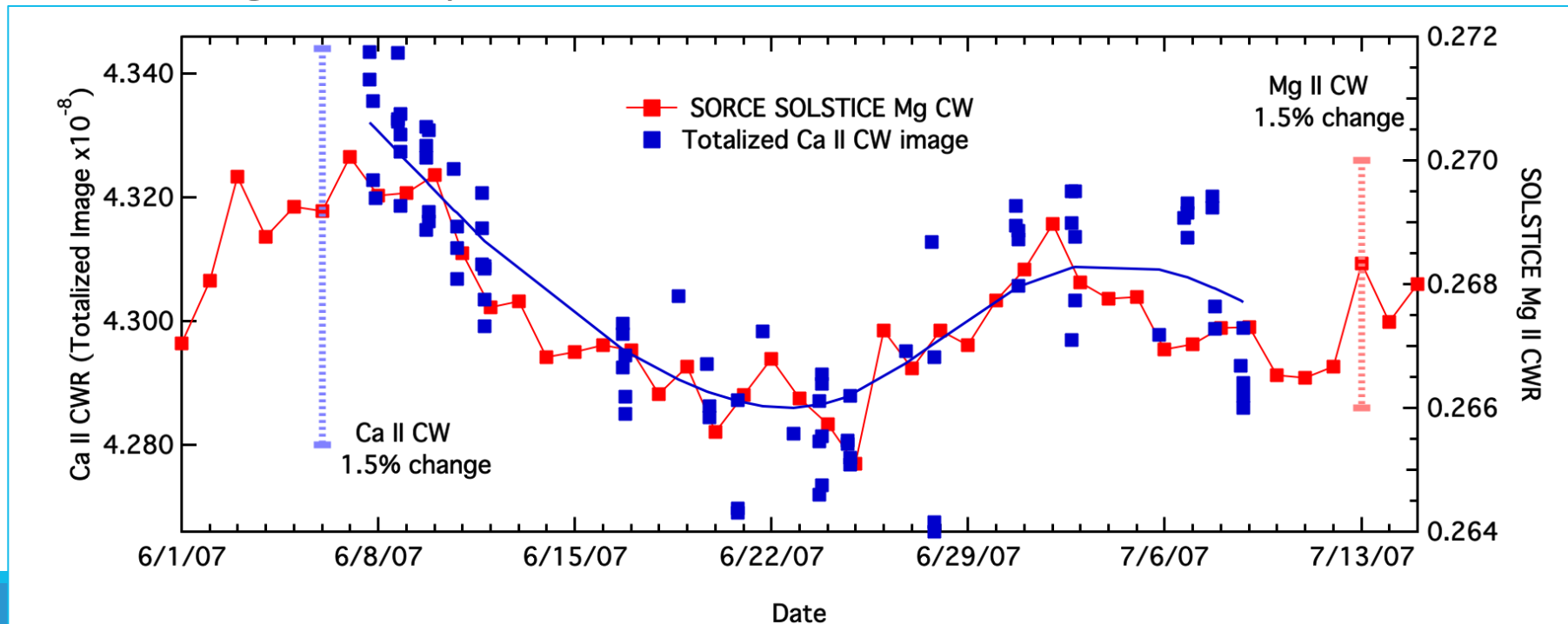
Core-to-Wing Imaging in Ca II

Most core-to-wing studies use the Sun as a star instead of analyzing every pixel

Ca II core-to-wing images are based on high contrast full disk observations

- This provides more physical information as an image vs. a set of numbers

However, to obtain Sun as a star data, a sum of the intensities across the solar disk is taken to give comparable data



Summary of Core-to-Wing Ratio Images

Narrow band filters provide high contrast – easier to determine bright contributions, i.e. facula, plage, as well as network structures

Construction of core-to-wing images emphasizes all these features

Available data covers extremely limited time series in Cycle 23

- These images would be very valuable during times of high activity and should be routinely measured

Future work - deconstruction of the Mg II proxy

An image can be used to produce the proxy – but the proxy can't be used to produce an image

Conclusion

Solar variability is an important but poorly understood component of the Earth climate system.

The relationship between solar irradiance and the activity within the Sun is complicated and nontrivial.

However, different layers of the solar atmosphere radiate differently and this can be captured with image processing.

Corrective image processing is essential for quality image analysis and advances in computer technology are required to match the advantages gained in image analysis.

Core-to-wing image analysis in Calcium II for an entire solar cycle could provide meaningful information about the solar irradiance.

Thank you!